Journal of Hydrology 535 (2016) 235–255

Contents lists available at ScienceDirect

Journal of Hydrology

journal homepage: www.elsevier.com/locate/jhydrol

Sea-level rise impacts on seawater intrusion in coastal aquifers: Review and integration

Hamed Ketabchi [a,*], Davood Mahmoodzadeh [b], Behzad Ataie-Ashtiani [b,c], Craig T. Simmons [c]

[a] Department of Water Resources Engineering, Tarbiat Modares University, PO Box 14115-336, Tehran, Iran
[b] Department of Civil Engineering, Sharif University of Technology, PO Box 11155-9313, Tehran, Iran
[c] National Centre for Groundwater Research & Training and School of the Environment, Flinders University, GPO Box 2100, Adelaide, South Australia 5001, Australia

ARTICLE INFO

Article history:
Received 17 November 2015
Received in revised form 23 January 2016
Accepted 27 January 2016
Available online 6 February 2016
This manuscript was handled by Geoff Syme, Editor-in-Chief

Keywords:
Climate change
Coastal aquifers
Groundwater
Sea-level rise
Seawater intrusion

SUMMARY

Sea-level rise (SLR) influences groundwater hydraulics and in particular seawater intrusion (SWI) in many coastal aquifers. The quantification of the combined and relative impacts of influential factors on SWI has not previously been considered in coastal aquifers. In the present study, a systematic review of the available literature on this topic is first provided. Then, the potential remaining challenges are scrutinized. Open questions on the effects of more realistic complexities such as gradual SLR, parameter uncertainties, and the associated influences in decision-making models are issues requiring further investigation.

We assess and quantify the seawater toe location under the impacts of SLR in combination with recharge rate variations, land-surface inundation (LSI) due to SLR, aquifer bed slope variation, and changing landward boundary conditions (LWBCs). This is the first study to include all of these factors in a single analysis framework. Both analytical and numerical models are used for these sensitivity assessments. It is demonstrated that (1) LSI caused by SLR has a significant incremental impact on the seawater toe location, especially in the flatter coasts and the flux-controlled (FC) LWBCs, however this impact is less than the reported orders of magnitude differences which were estimated using only analytical solutions; (2) LWBCs significantly influence the SLR impacts under almost all conditions considered in this study; (3) The main controlling factors of seawater toe location are the magnitudes of fresh groundwater discharge to sea and recharge rate. Regional freshwater flux entering from the landward boundary and the groundwater hydraulic gradient are the major contributors of fresh groundwater discharge to sea for both FC and head-controlled (HC) systems, respectively; (4) A larger response of the aquifer and larger seawater toe location changes are demonstrable for a larger ratio of the aquifer thickness to the aquifer length particularly in the HC systems; (5) The lowest sensitivity of seawater toe location is found for the density difference ratio of the seawater and freshwater, and also for the aquifer bed slope; (6) The early-time observations show seawater fingers below the inundated lands due to SLR which are diminished and ultimately extinguished; and (7) A less than 2% reversal effect on the seawater toe location after overshoot mechanism is observed in the transient simulations which suggests that this mechanism is an insignificant and impractical factor compared to other more significant factors.

1. Introduction

Groundwater is generally the most important freshwater resource in many coastal regions which are threatened by seawater intrusion (SWI) (Ataie-Ashtiani and Ketabchi, 2011; Ketabchi and Ataie-Ashtiani, 2015b). Climate change impacts such as sea-level rise (SLR) and precipitation variations that change recharge rates are the influential climatic factors that affect SWI (Werner et al., 2013; Ataie-Ashtiani et al., 2013a). The Intergovernmental Panel on Climate Change (IPCC, 2013) predicts that the global mean SLR may rise between 0.26 m and 0.82 m by the year 2100. A SLR in the range of 0.18–0.59 m was predicted by IPCC (2007) for a similar period. This shows a significant upward revision for SLR prediction between IPCC (2007) and IPCC (2013) and highlights the potential importance of SLR impacts on SWI.

Based on the assessments of IPCC (2013), annual mean precipitation can vary up to ±50% in the world. This range includes the

* Corresponding author. Tel.: +98 21 4829 2316; fax: +98 21 4829 2200.
E-mail addresses: h.ketabchi@modares.ac.ir (H. Ketabchi), dmahmoodzadeh@alum.sharif.edu (D. Mahmoodzadeh), ataie@sharif.edu (B. Ataie-Ashtiani), craig.simmons@flinders.edu.au (C.T. Simmons).

http://dx.doi.org/10.1016/j.jhydrol.2016.01.083

Nomenclature

SWI	seawater intrusion
SLR	sea-level rise
LSI	land-surface inundation
LWBCs	landward boundary conditions
FC	flux-controlled
HC	head-controlled
HYP	hypothetical aquifer
REAL	real-case aquifer
EXP	experimental-test aquifer
MSL	mean sea level
OoM	order of magnitude
R	ratio parameter to quantify the influence of LSI on SLR-induced SWI
X^s_{Toe}	seawater toe location for post SLR with LSI condition
X^v_{Toe}	seawater toe location for post SLR without LSI condition
X^0_{Toe}	seawater toe location prior to SLR
ΔX_{Toe}	seawater toe changes
X_{Toe}	seawater toe location
X^*_{Toe}	dimensionless seawater toe location
h	hydraulic head
h^*	dimensionless hydraulic head
x	distance taken from the coastline
x^*	dimensionless distance taken from the coastline
dh/dx	hydraulic gradient
K	hydraulic conductivity
h_{LW}	landward hydraulic head
h^*_{LW}	dimensionless landward hydraulic head
h_{SW}	seaward hydraulic head
h^c_{SW}	corrected seaward hydraulic head
h^*_{SW}	dimensionless seaward hydraulic head
Δh_{SW}	sea-level rise value
Δh^*_{SW}	dimensionless sea-level rise value
L	aquifer length
L_{div}	hydraulic divide location
L^*_{div}	dimensionless hydraulic divide location
B	average aquifer thickness
B^*	dimensionless average aquifer thickness
W	recharge rate
W^*	dimensionless recharge rate
Q_f	fresh groundwater discharge to sea
Q^*_f	dimensionless fresh groundwater discharge to sea
q_b	regional flux entered from landward boundary
q^*_b	dimensionless regional flux entered from landward boundary
δ	density difference ratio of the seawater and freshwater
δ^c	corrected density difference ratio of the seawater and freshwater
ρ_s	seawater density
ρ_f	freshwater density
C_s	seawater concentration
C_f	freshwater concentration
μ	fluid dynamic viscosity
D_m	molecular diffusion
S_s	specific storage
φ	angle of impervious aquifer bed against the horizontal
α_L	longitudinal dispersivity
α_T	transverse dispersivity
ξ_0	depth of the interface below the water table outcrop at the coast
χ_0	width of the gap through the submarine outflow
S	land-surface slope
g	gravitational acceleration
t	time
t^*	dimensionless time
ε	effective porosity

estimate of projected uncertainties. The high latitudes and the equatorial Pacific Ocean are likely to experience an increase in annual mean precipitation by the end of this century. In many mid-latitude and subtropical arid regions, mean precipitation will likely decrease, while in many mid-latitude wet regions, mean precipitation will likely increase by the year 2100 (IPCC, 2013; Horton et al., 2014; Bring et al., 2015). Larger uncertainties surround the projections of surface runoff and recharge rate to groundwater resources, which are affected by many climatic factors, include changes in mean precipitation and temperature regimes. Further assessments have been provided by e.g. Holman (2006), IPCC (2013), and Bring et al. (2015).

Ketabchi and Ataie-Ashtiani (2015b,c) developed the efficient and robust decision models which have the superior abilities in terms of both solution quality and computational time criteria. Using such decision models, they highlighted a need for an integrated study to address how the conceptualization of climate change impacts e.g. SLR, land-surface inundation (LSI), and recharge rate variations can be handled on prospective coastal groundwater management strategies. Gorelick and Zheng (2015) emphasized that global changes such as climatic effects led to multiple stresses that should be considered in groundwater management plans. Ojha et al. (2015) assessed the long-term potential influences of climate change, e.g. SLR impacts in aquifers and efficient management of these resources in many regions of the world. They concluded that such studies are yet open challenges concerning uncertainties in modeling and in defining climate change scenarios, heterogeneities, estimation of recharge rate to groundwater systems, data challenges, and addressing the increasing threats from competing demands and mounting hydrologic stresses on groundwater systems, which all indicated a pressing need to develop effective management strategies.

The main objective of this study is to provide a systematic review of numerous previous studies and to then undertake an analysis of the relative importance of the purported influential factors controlling SWI. We present the literature review in tabulated and diagrammatic formats so as to be easily comprehensible and to easily identify what factors previous studies have and have not included. This is the first study that highlights the impacts of all of known SLR-induced influential factors and thus directs us to evaluate the relative importance of these impacts on SWI using both analytical and numerical methods. The SLR impacts on the SWI interface and in particular seawater toe location are the focus of this study. Such an integrated assessment does not exist because each previous study has only assessed a (different) subset of the purported controlling factors.

2. A review of previous studies

In recent years, there has been a growing body of research relating to climatic and hydrogeologic controls on SWI. It is not easy to rapidly discern the similarities and differences in these studies. Furthermore, it is also not immediately clear where current knowledge gaps might exist. Even more importantly, it is not indeed evident that any previous studies have conducted an integrated assessment to analyze the relative importance of the purported range of influential factors.

Recently, Ketabchi et al. (2014) presented an extensive review and study on the influence of SLR on fresh groundwater lenses of small islands. They concluded that fresh groundwater lens status was most sensitive to recharge rate, followed by land-surface slope, aquifer layer thickness, and hydraulic conductivity in comparison with the vertical movement of SLR, in the range of parameters considered in their study. Mahmoodzadeh et al. (2014) numerically investigated the combined impacts of SLR, associated LSI, and variations in recharge rate on the fresh groundwater lens salinization of Kish Island, Iran. Their results also demonstrated that the impacts of LSI caused by SLR and recharge rate variations were more important than the estimated SLR impacts without LSI.

We focus here on a review and evaluation of coastal aquifer systems. Fig. 1 illustrates two conceptual models of sloping unconfined coastal aquifers. Fig. 1a and b illustrate SWI in a coastal aquifer prior to and after SLR in a flux-controlled (FC) system. In this system, the regional groundwater discharge to the sea is constant and controls the status of SWI. In Fig. 1c and d, the landward boundary conditions (LWBCs) considered is head-controlled (HC). In this system, the water table position at the landward boundary is constant despite SLR. Fig. 1c and d shows the SWI status, prior to and after SLR condition, respectively. LSI arising from the landward movement of the coastline, accompanying SLR is shown in all conceptual models and is obviously dependent upon the land-surface slope.

Table 1 provides a summary of the recent studies based on the modeling methods and the processes that have been considered. Both analytical solutions (e.g. Werner and Simmons, 2009; Ataie-Ashtiani et al., 2013a; Carretero et al., 2013; Koussis et al., 2015) and numerical simulations (e.g. Watson et al., 2010; Chang et al., 2011; Laattoe et al., 2013; Sefelnasr and Sherif, 2014) have been used for the analysis of SLR impacts on SWI. The application of analytical solutions to estimate the location of seawater toe needs many simplifications such as steady-state conditions, sharp freshwater-seawater transition zones, and one-dimensional flow.

Based on the review of the previous studies, a variety of simulation assumptions is summarized in Table 1, including; sharp (e.g. Koussis et al., 2012) and disperse (e.g. Yechieli et al., 2010) interface approaches, two-dimensional (e.g. Kooi et al., 2000) and three-dimensional (e.g. Sefelnasr and Sherif, 2014) simulations, steady-state (e.g. Ataie-Ashtiani et al., 2013a) and transient (e.g. Morgan et al., 2015) simulations, and fully saturated (e.g. Chang et al., 2011) and saturated/unsaturated domains (e.g. Loaiciga et al., 2012). Aquifer hydrogeological properties are generally heterogeneous (Werner et al., 2013). As can be recognized in Table 1, the assumption of a single-layer system as a homogeneous aquifer was considered in most of the previous studies (e.g. Sherif and Singh, 1999; Michael et al., 2013; Chesnaux, 2015; Koussis et al., 2015) while there were the limited studies which considered the heterogeneous coastal aquifers as two-layer (e.g. Kooi et al., 2000) and multi-layer (e.g. Stigter et al., 2014) systems.

Table 1 confirms that none of the previous studies have considered the combined effects of SLR, LSI, variations in recharge rate, aquifer bed slope, and LWBCs on SWI in coastal aquifers. Therefore, the importance and the necessity of further research in the field of these impacts are recognized on these coastal aquifers. In this

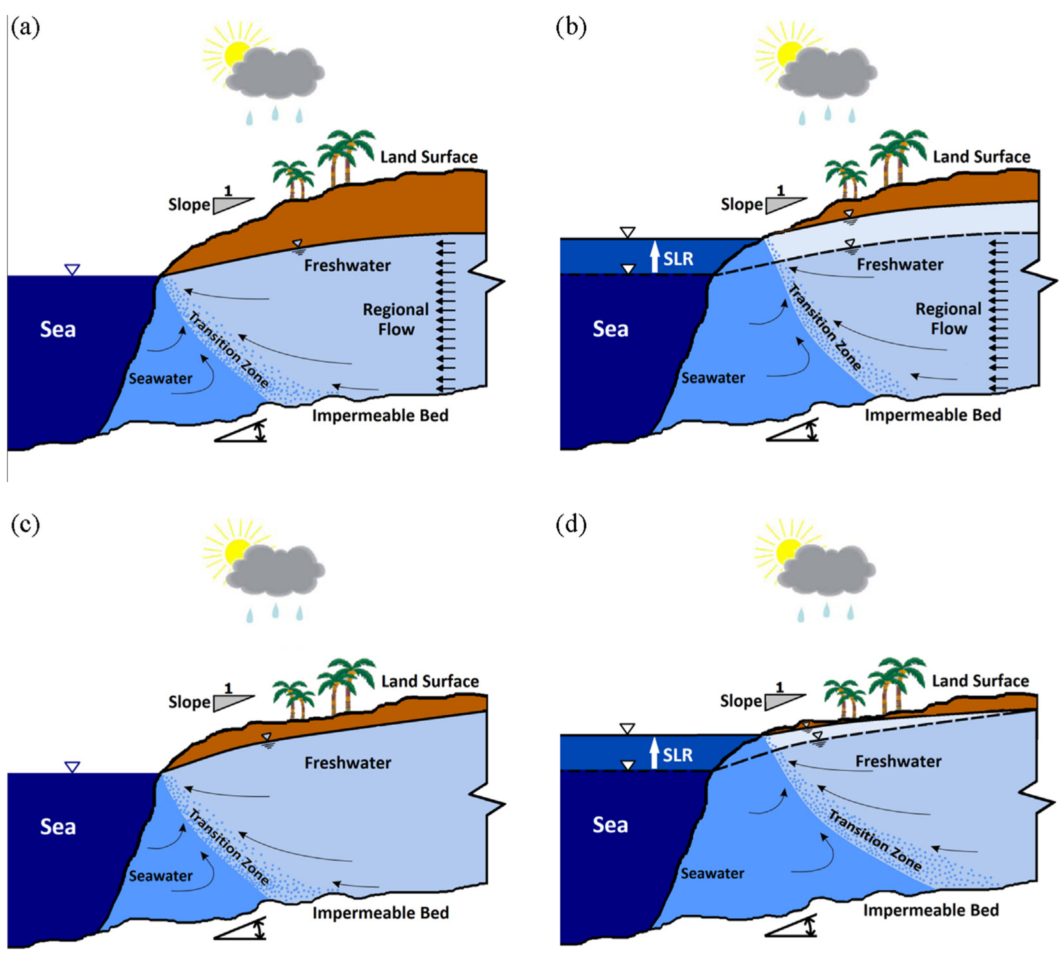

Fig. 1. Conceptual model of a sloping unconfined coastal aquifer system used for investigating the impacts of SLR on SWI: (a) the FC system prior to SLR, (b) the FC system after SLR, (c) the HC system prior to SLR, and (d) the HC system after SLR.

Table 1
Summary of studies relating to SLR-induced impacts in coastal aquifers.

References	Simulation[a]	Application[b]	Assessed processes[c]						
			SLR	LSI	BS	W	LWBCs	OSH	FIN
Sherif and Singh (1999)	NU (FED), 2D, CO, SCO, SL, SS, SAT	REAL	**Yes** 0.2 m, 0.5 m (I)	–	**Yes** 0.3%	–	HC	–	–
Kooi et al. (2000)	AN, NU (METROPOL-3), IF, DD, 2D, UNCO, SL, TL, T, SAT	HYP	**Yes** 0.1–1 mm/year (G)	**Yes** 0.1%	–	–	HC	–	**Yes**
Feseker (2007)	NU (SWIMMOC), DD, 2D, TL, T, SAT	HYP*	**Yes** 0.5 m/century	–	–	**Yes**	FC	–	–
Giambastiani et al. (2007)	NU (MOCDENS3D), DD, 2D, UNCO, ML, SS, T, SAT	REAL	**Yes** 0.475–0.9 m/century (G)	–	–	**Yes**	HC	–	–
Werner and Simmons (2009)	AN, IF, 2D, UNCO, SL, SS, SAT	HYP*	**Yes** 0.1–1.5 m (I)	–	–	**Yes**	**Yes** FC, HC	–	–
Carneiro et al. (2010)	NU (FEMWATER), DD, 3D, UNCO, ML, T, UNSAT	REAL	**Yes** 0.18–0.59 m (G)	**Yes**	–	**Yes**	FC, HC	–	–
Oude Essink et al. (2010)	NU (MOCDENS3D), DD, 3D, CO, ML, T	REAL	**Yes** 0.85–2 m (G)	**Yes**	–	**Yes**	HC	–	–
Watson et al. (2010)	AN, NU (FEFLOW), IF, DD, 2D, UNCO, SL, SS, T, UNSAT	HYP	**Yes** 1 m (I)	–	–	–	FC	**Yes**	–
Yechieli et al. (2010)	NU (FEFLOW), DD, 2D, UNCO, ML, SS, T, UNSAT	REAL	**Yes** 10 mm/year (G)	**Yes** 0.25%	**Yes** ~0.9%	**Yes**	FC	–	–
Chang et al. (2011)	NU (SEAWAT), DD, 2D, CO, UNCO, SL, T, SAT	HYP*	**Yes** 0.2–4 m (I); 0.04–1 mm/year (G)	–	–	**Yes**	FC	**Yes**	–
Webb and Howard (2011)	NU (SEAWAT), DD, 2D, UNCO, SL, T, SAT	HYP*	**Yes** 0.1–1.5 m (G)	–	–	**Yes**	HC	–	–
Loaiciga et al. (2012)	NU (FEFLOW), DD, 3D, UNCO, SL, SS, UNSAT	REAL	**Yes** 5, 10 mm/year (G)	**Yes**	–	**Yes**	–	–	–
Chang and Clement (2012)	NU (SEAWAT), DD, 2D, UNCO, SL, T, SAT	HYP	–	–	–	**Yes**	FC	–	–
Werner et al. (2012)	AN, IF, 2D, CO, UNCO, SL, SS, SAT	HYP*	**Yes** 1 m (I)	–	–	**Yes**	**Yes** FC, HC	–	–
Koussis et al. (2012)	AN, IF, 2D, UNCO, SL, SS, SAT	HYP*	**Yes** 1 m (I)	–	**Yes** ~1.7%	**Yes**	FC	–	–
Ataie-Ashtiani et al. (2013a)	AN, IF, 2D, UNCO, SL, SS, SAT	HYP*	**Yes** 2 m (I)	**Yes** 1%, 10%	–	**Yes**	**Yes** FC, HC	–	–
Laattoe et al. (2013)	NU (FEFLOW), DD, 2D, UNCO, SL, T, SAT	HYP	**Yes** 0, 1 m (I); 10 mm/year (G)	**Yes** 0.1%–0.4%	–	–	**Yes** FC, HC	–	**Yes**
Morgan et al. (2013)	EXP, NU (FEFLOW), DD, 2D, UNCO, SL, T, UNSAT	EXP	**Yes** 0.024 m (I)	**Yes** 75.4%	–	–	FC	**Yes**	–
Michael et al. (2013)	NU (SUTRA), DD, 2D, UNCO, SL, SS, SAT	HYP	**Yes** 1 m (I)	–	–	**Yes**	FC	–	–
Carretero et al. (2013)	AN, IF, 2D, UNCO, SL, SS, SAT	REAL	**Yes** 1 m (I)	–	–	**Yes**	**Yes** FC, HC	–	–
Lu and Werner (2013)	NU (SEAWAT), DD, 2D, CO, SL, T, SAT	HYP*	**Yes** 1 m (I)	–	–	–	HC	**Yes**	–
Mazi et al. (2013)	AN, IF, 2D, UNCO, SL, SS, SAT	HYP	**Yes** 0.59 m, 1.6 m (I)	–	**Yes** ~±1%	–	**Yes** FC, HC	–	–
Mazi et al. (2014)	AN, IF, 2D, UNCO, SL, SS, SAT	REAL	–	–	**Yes** 1%, 0.3%, 0.4%, 1.7%		**Yes** FC, HC	–	–
Sefelnasr and Sherif (2014)	NU (FEFLOW), DD, 3D, SCO, ML, SS, UNSAT	REAL	**Yes** 0.5 m, 1 m (I)	**Yes**	–	–	HC	–	–
Stigter et al. (2014)	NU (FEN), 2D, ML, T	REAL	**Yes** 1 m (I)	–	–	**Yes**	HC	–	–
Luoma and Okkonen (2014)	NU (MODFLOW and UZF1), IF, 3D, UNCO, SL, T, UNSAT	REAL	**Yes** 0.09–0.51 m (G)	**Yes**	–	**Yes**	FC	–	–
Green and MacQuarrie (2014)	NU (SEAWAT), DD, 2D, UNCO, ML, SS, T, UNSAT	REAL	**Yes** 0.93 m, 1.86 m (I)	–	–	**Yes**	HC	–	–
Lu et al. (2015)	AN, IF, 2D, CO, UNCO, SL, SS, SAT	HYP	**Yes** 1 m (I)	–	–	–	**Yes** FC, HC, GH	–	–
Chesnaux (2015)	AN, IF, 2D, CO, UNCO, SL, SS, SAT	HYP	**Yes** 0–2 m (I)	**Yes** 3.5%–∞	–	**Yes**	FC	–	–
Koussis et al. (2015)	AN, NU (FEFLOW), IF, DD, 1D, 2D, UNCO, SL, SS, UNSAT	HYP*	**Yes** 1 m (I)	–	**Yes** 1%, 0.3%, 0.5%	**Yes**	FC, HC	–	–
Morgan et al. (2015)	NU (MODFLOW), DD, 2D, CO, UNCO, SL, T, SAT, UNSAT	HYP	**Yes** 1 m (I); 10 mm/year (G)	–	–	–	**Yes** FC, HC	**Yes**	–

[a] IF: sharp-interface flow; DD: density-dependent (disperse) flow; D: dimension; UNCO: unconfined; CO: confined; SCO: semi-confined; SS: steady-state; T: transient; AN: analytical; EXP: experimental; NU: numerical; SL: single-layer; TL: two-layer; ML: multi-layer, SAT: fully saturated modeling; UNSAT: saturated/unsaturated modeling.
[b] HYP: hypothetical aquifer; HYP*: hypothetical aquifer with real-case data; REAL: real-case aquifer; EXP: experimental-test aquifer.
[c] SLR: sea-level rise; LSI: land-surface inundation; BS: aquifer bed slope; W: recharge rate; LWBCs: landward boundary conditions; OSH: overshoot; FIN: seawater finger; I: instantaneous; G: gradual; FC: flux-controlled system; HC: head-controlled system; GH: general-head.

study, sloping aquifers are aquifers in which the land surface and/or the aquifer impervious bed have an angle that dips away from the horizontal (e.g. Ataie-Ashtiani et al., 2013a). Some previous studies such as Kooi et al. (2000) and Mazi et al. (2013) have used this term to define aquifers with only an inclined bed boundary.

In the following, more explanations regarding the summarized studies in Table 1 are provided while an insightful analysis of the relative importance of the SLR-induced phenomena and the associated impacts is undertaken. We have categorized our review to: (1) the impacts of SLR and LSI caused by SLR on sloping coastal aquifers; (2) the impacts of LWBCs on SWI due to SLR; (3) the impacts of aquifer bed slope on SLR-induced SWI; and (4) overshoot and seawater fingering phenomena due to SLR. The modeling approaches and the methodologies considered in the previous studies are also discussed.

2.1. SLR and LSI impacts

The studies of Sherif and Singh (1999) and Kooi et al. (2000) are the first predictive studies of SLR impacts on SWI in coastal aquifers. As can be recognized in Table 1, the instantaneous SLR assumption has been implemented in most previous studies (e.g. Werner and Simmons, 2009; Yechieli et al., 2010; Watson et al., 2010; Chang et al., 2011; Koussis et al., 2012, 2015; Ataie-Ashtiani et al., 2013a; Mazi et al., 2013; Chesnaux, 2015). The assumption of instantaneous SLR is a simplification considered in the modeling procedure, which causes the estimated SWI is more rapid than would occur due to gradual SLR (Watson et al., 2010). This is a simplification considered in the modeling procedure, allowing for gradual SLR to investigate SLR impacts with a greater level of realism (Watson et al., 2010). There are very limited works such as Laattoe et al. (2013) and Morgan et al. (2015) which have investigated both instantaneous and gradual SLR impacts, mostly focusing on the temporal aspects and phenomena such as the overshoot mechanism.

In a short review, Ataie-Ashtiani et al. (2013a) showed that most of the recent research on SLR impacts on SWI in coastal aquifers, neglected LSI in their studies. They showed that only a very limited number of studies (Kooi et al., 2000; Loaiciga et al., 2012; Rotzoll and Fletcher, 2012; Ferguson and Gleeson, 2012) had considered this impact. It is immediately apparent in Table 1 that investigations on the impacts of LSI are rather limited.

Ataie-Ashtiani et al. (2013a) defined the dimensionless ratio parameter of $R = (X^s_{\mathrm{Toe}} - X^v_{\mathrm{Toe}})/(X^v_{\mathrm{Toe}} - X^0_{\mathrm{Toe}})$ to quantify the influence of LSI on SLR-induced SWI, where X^s_{Toe} and X^v_{Toe} are seawater toe locations for conditions of post SLR with LSI and without LSI, respectively, and X^0_{Toe} is the seawater toe location prior to SLR. Larger magnitudes of R characterize a more significant impact of LSI on SWI. Using a simple analytical solution for calculation of R, Ataie-Ashtiani et al. (2013a) showed that the influence of LSI on SWI could be an order of magnitude (OoM) larger than vertical SLR when a land-surface slope of 1% was considered. Also, the impact of LSI on the seawater toe location was of the same OoM as the impacts of vertical SLR for the cases with the slope of 10%. For example, the Gaza aquifer, Palestine, with land-surface slopes of infinite (i.e. vertical coast), 10% and 1% was investigated by Ataie-Ashtiani et al. (2013a). The parameters employed were taken from Moe et al. (2001) and Werner et al. (2012). Under the worst conditions tested for the Gaza aquifer with the land-surface slope of 1%, using a simple analytical solution, Ataie-Ashtiani et al. (2013a) showed that the calculated R could be 10.6 for FC LWBCs while the R of 3.4 could be obtained for similar condition where the LWBC was treated as a HC boundary. Therefore, Ataie-Ashtiani et al. (2013a) highlighted that the influence of LSI is a significant controlling factor on SWI status caused by SLR.

Recently, Chesnaux (2015) presented four closed-form analytical solutions for rapid calculations estimating the impacts of SLR on coastal aquifers and conducted a number of sensitivity analyses on the critical parameters involved in the equations. He showed that the land-surface slope is an important factor which controls the magnitude of the SLR impacts which is in agreement with a highlighted finding of Ataie-Ashtiani et al. (2013a). The results of Sefelnasr and Sherif (2014) also showed that ignoring the impacts of LSI causes an underestimation of the possible consequences of SLR when compared to results of Werner and Simmons (2009). Although some studies such as Ataie-Ashtiani et al. (2013a), Mahmoodzadeh et al. (2014), and Chesnaux (2015) have highlighted that LSI is an important factor which controls the impacts of SLR on coastal aquifers, it has not been investigated in some recent studies in this area (e.g. Michael et al., 2013; Mazi et al., 2014; Lu et al., 2015; Koussis et al., 2015; Morgan et al., 2015).

SLR-LSI impacts have also been considered in combination with the impact of recharge rate variations in some previous studies such as Carneiro et al. (2010), Ataie-Ashtiani et al. (2013a), and Sefelnasr and Sherif (2014). A reduction in recharge rate is expected to occur with climate change in arid coastal regions which experience considerable variations in annual recharge rates (e.g. Sefelnasr and Sherif, 2014; Carneiro et al., 2010). Sefelnasr and Sherif (2014) showed in the Nile Delta Aquifer, Egypt that a SLR of 1 m and a 2.3 billion m^3/year reduction in net recharge (drier scenario) caused a considerable reduction in the fresh groundwater volume from 883 km^3 to 513 km^3 (i.e. 41.9% reduction). When the rate of base net recharge was kept constant, a fresh groundwater volume of 748 km^3 was predicted (i.e. 15.3% reduction). Also, a 1.15 billion m^3/year increase in net recharge rate (wetter scenario) in addition to 1 m SLR gave rise to 781 km^3 of fresh groundwater (i.e. 11.5% reduction). Carneiro et al. (2010) also confirmed the increasing impacts of SLR and recharge rate reduction in the Saidia aquifer, Mediterranean coast of Morocco, using the scenarios of 0.18 m, 0.35 m, and 0.59 m SLR and 9%, 19%, and 47% reduction of recharge rate.

2.2. LWBCs impacts on SWI due to SLR

The importance of the influence of LWBCs on groundwater hydraulics and SWI in coastal aquifers were highlighted for the first time in the works of Ataie-Ashtiani et al. (1999, 2001). They investigated two main classifications of FC and HC for LWBCs of the coastal aquifer. Using numerical simulations for investigating the impacts of tidal fluctuations on coastal groundwater, Ataie-Ashtiani et al. (1999, 2001) showed that where the LWBCs were HC, the effects of tidal fluctuations on SWI were more pronounced than for the FC cases. They further showed that when the LWBCs were HC, the over-height in the water table as a result of the tidal fluctuation had a significant effect on groundwater discharge to the sea (Ataie-Ashtiani et al., 2001; Ataie-Ashtiani, 2015). As summarized in Table 1, the studies of Werner and Simmons (2009), Ataie-Ashtiani et al. (2013a), Carretero et al. (2013), Michael et al. (2013), Laattoe et al. (2013), Mazi et al. (2013), and Morgan et al. (2015) have studied the importance of LWBCs on SWI due to SLR.

FC systems support much higher hydraulic gradients than found in HC ones because the hydraulic head on the landward boundary can rise in response to a rise on the seaward boundary. HC systems will experience a reduction in fresh groundwater discharge compared to FC systems due to a reduced hydraulic gradient (Werner et al., 2012; Michael et al., 2013). This pattern is seen in Fig. 2, which contains a plot of SLR ratio vs. hydraulic gradient for some of the coastal aquifers summarized in Table 1. Hydraulic gradient (dh/dx) shown in Fig. 2, is estimated by

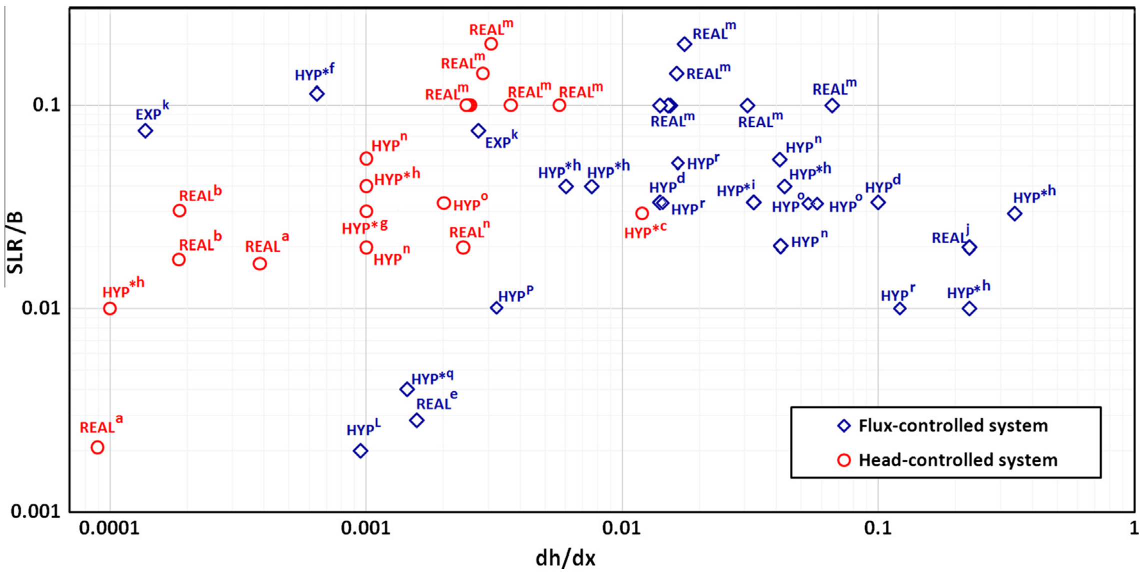

Fig. 2. Hydraulic gradient vs. SLR for several coastal aquifers. HYP: hypothetical aquifer; HYP*: hypothetical aquifer with real-case data; REAL: real-case aquifer; EXP: experimental-test aquifer; [a]Nile Delta aquifer, Egypt and Madras aquifer, India (Sherif and Singh, 1999); [b]Ravenna Aquifer, Italy (Giambastiani et al., 2007); [c]Nile Delta aquifer, Egypt (Werner and Simmons, 2009); [d]Hypothetical aquifer (Watson et al., 2010); [e]Mediterranean Aquifer (Yechieli et al., 2010); [f]Pioneer Valley Aquifer, Australia (Chang et al., 2011); [g]Poineer Valley Aquifer, Australia (Webb and Howard, 2011); [h]Gaza aquifer, Palestine, Pioneer Valley, Australia, and Uley South, Australia (Werner et al., 2012); [i]Mediterranean Aquifer (Koussis et al., 2012); [j]Gaza aquifer, Palestine (Ataie-Ashtiani et al., 2013a); [k]Hypothetical aquifer and experimental-test aquifer (Morgan et al., 2013); [l]Hypothetical aquifer (Michael et al., 2013); [m]Partido de La Costa aquifer, Argentina (Carretero et al., 2013); [n]Hypothetical aquifer (Mazi et al., 2013); [o]Hypothetical aquifer (Lu et al., 2015); [p]Hypothetical aquifer (Chesnaux, 2015); [q]Mediterranean Aquifer (Koussis et al., 2015); [r]Hypothetical aquifer (Morgan et al., 2015).

$Q_f/(\mathrm{B}K)$ for FC systems and $(h_{\mathrm{LW}} - h_{\mathrm{SW}})/L$ for HC systems, where h [L] is hydraulic head, x [L] is distance, taken from the coastline, K [L T^{-1}] is hydraulic conductivity, h_{LW} [L] is landward hydraulic head, h_{SW} [L] is seaward hydraulic head, L [L] is aquifer length, B [L] is aquifer thickness, and Q_f [L^2 T^{-1}] is fresh groundwater discharge to sea which is $(q_b + WL)$. q_b [L^2 T^{-1}] is regional freshwater flux entering from landward boundary and W [L T^{-1}] is recharge rate from land surface in this equation. As shown in Fig. 2, the main tendency is that FC systems have a higher dh/dx relative to HC systems. Some FC coastal aquifers show minor dh/dx such as aquifers considered by Chang et al. (2011), Michael et al. (2013), and Morgan et al. (2013). The main reasons for small dh/dx in these FC systems are low Q_f due to low W and thus low q_b in LWBCs. The cases of Chang et al. (2011) are aquifers with low W and q_b. The recharge rate of coastal aquifers considered by Morgan et al. (2013) was zero. Michael et al. (2013) implemented no regional flux for their coastal aquifer analysis.

The ratio of seawater toe location changes (ΔX_{Toe}) caused by SLR to aquifer length (L) versus SLR to aquifer thickness (B) is shown in Fig. 3 for the coastal aquifers of Table 1. As can be seen from Fig. 3, the HC systems are more vulnerable than the FC systems for SLR-induced SWI because dh/dx between landward and seaward boundary conditions cannot be maintained (Ataie-Ashtiani et al., 2013a; Michael et al., 2013).

Werner and Simmons (2009) applied a simple analytical solution to study the importance of LWBCs on SWI due to SLR, for the first time. They showed that the choice of LWBCs was an important factor in SLR-induced SWI. They investigated SLR of 0.1–1.5 m under typical values of the recharge rate, the hydraulic conductivity, and the aquifer depth and observed that under FC LWBCs, seawater toe location was enhanced no larger than 50 m. However in HC cases, the magnitude of seawater toe location changes was on the order of hundreds of meters for the same SLR (Fig. 3). They did not consider the effect of variations in the recharge rate and LSI according to land-surface slope in their work.

Carretero et al. (2013) used a simple analytical solution in a similar manner as Werner and Simmons (2009), and investigated the impacts of a potential 1 m SLR on the coast of Partido de La Costa, Argentina. They also assessed the influence of both above-mentioned LWBCs on SLR-induced SWI and obtained similar results in terms of the importance of LWBCs-related behaviors of the coastal aquifer in response to SLR. Carretero et al. (2013) found that the larger variations of seawater toe location changes were observed with variations in the recharge rate under FC LWBCs. Their results were obtained by applying the specific characteristics of Partido de La Costa, Argentina coastal aquifer. When the recharge rate was set to 230 mm/year, the seawater intruded 25 m landward due to a 1 m SLR while reducing the recharge rate to 194 mm/year (reduction of 14.3%) led to a seawater toe location of 38 m (52% increase) as the maximum value forecast in the FC scenarios of their study. In the HC scenarios more extensive SWI in excess of 200 m compared to the FC cases was estimated for recharge rates of 230 mm/year and 194 mm/year. The seawater intruded inland 193 m and 211 m (increase of 9.3%), respectively for a 1 m SLR. Differences between the FC and the HC tests in response to both SLRs and recharge rate variations were found to be in agreement with the Werner and Simmons (2009) study. Rotzoll and Fletcher (2012), Loaiciga et al. (2012) and Rasmussen et al. (2013) also observed that variations in the net recharge rate were the dominant factors in SWI under FC LWBCs, but did not consider the influence of LSI caused by SLR. Their results confirmed the minor response of HC cases to variations in recharge rate. Also, the large SWI under such HC systems was observed by Werner and Simmons (2009) compared to FC systems.

Laattoe et al. (2013) extended the work of Werner and Simmons (2009) by considering LSI impacts and obtained comparable results using numerical simulations. They adopted the simplified unconfined coastal aquifer of Kooi et al. (2000) for a range of SWI scenarios. They showed that the SWI caused by LSI and the associated intrusion due to free convection emerge to be relatively insensitive to the choice of LWBCs, which is different from the findings of SLR-SWI studies that neglect LSI (e.g. Werner and Simmons, 2009). They also found that neglecting the effects of LSI on SWI caused a significant underestimation of seawater toe location. Laattoe

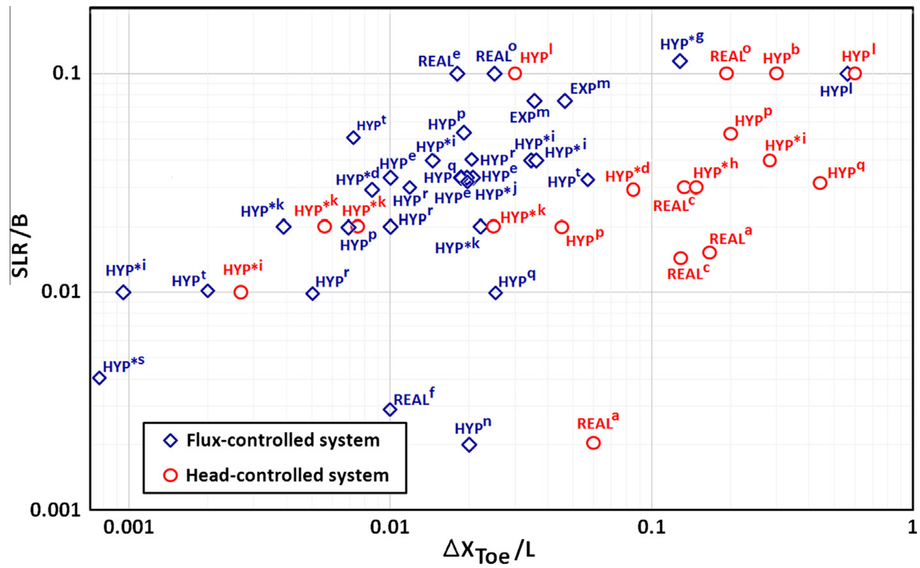

Fig. 3. Seawater toe location changes vs. SLR for several coastal aquifers. HYP: hypothetical aquifer; HYP*: hypothetical aquifer with real-case data; REAL: real-case aquifer; EXP: experimental-test aquifer. [a]Nile Delta aquifer, Egypt and Madras aquifer, India (Sherif and Singh, 1999); [b]Hypothetical aquifer (Kooi et al., 2000); [c]Ravenna Aquifer, Italy (Giambastiani et al., 2007); [d]Nile Delta aquifer, Egypt (Werner and Simmons, 2009); [e]Hypothetical aquifer (Watson et al., 2010); [f]Mediterranean Aquifer (Yechieli et al., 2010); [g]Pioneer Valley Aquifer, Australia (Chang et al., 2011); [h]Pioneer Valley Aquifer, Australia (Webb and Howard, 2011); [i]Gaza aquifer, Palestine, Pioneer Valley, Australia, and Uley South, Australia (Werner et al., 2012); [j]Mediterranean Aquifer (Koussis et al., 2012); [k]Gaza aquifer, Palestine (Ataie-Ashtiani et al., 2013a); [l]Hypothetical aquifer (Laattoe et al., 2013); [m]Hypothetical aquifer and experimental-test aquifer (Morgan et al., 2013); [n]Hypothetical aquifer (Michael et al., 2013); [o]Partido de La Costa aquifer, Argentina (Carretero et al., 2013); [p]Hypothetical aquifer (Mazi et al., 2013); [q]Hypothetical aquifer (Lu et al., 2015); [r]Hypothetical aquifer (Chesnaux, 2015); [s]Mediterranean Aquifer (Koussis et al., 2015); [t]Hypothetical aquifer (Morgan et al., 2015).

et al. (2013) observed little differences in the seawater toe location due to LSI impact for FC systems in comparison with HC systems. Laattoe et al. (2013) explained their reason to observations that in the simulation with LSI, inflows and outflows from coastal aquifer were almost entirely through the inundated land surface boundary and therefore the influence of LWBCs had little bearing on the flow trends. The impacts of recharge rate variations were not considered in their study. Clearly, the inclusion of different physical processes in an SWI analysis has a significant bearing on the dominant factors controlling the SWI process. Therefore, the choice of conceptual model will be a strong determinant on the results and the relative effects of model parameterization and LWBCs in any given conceptualization.

Ataie-Ashtiani et al. (2013a) developed a simple analytical solution to include LSI into SLR impacts on SWI. Both forms of LWBCs were included in their solution. It was shown that in some of the cases, LSI causes a negative flux and unstable interface of SWI and as the interface reached the inland and a steady-state condition cannot be calculated. It was shown that the worst SWI conditions and the seawater toe location were observed when LWBC was HC and it was combined with LSI.

Michael et al. (2013) used SUTRA to develop a two-dimensional model for assessing the effect of SLR on SWI in two types of groundwater systems that identified as recharge-limited (i.e. FC at upper boundary) and topography-limited (i.e. HC at upper boundary). Whereas global analysis indicated that more than half of the world coasts are topography-limited, they showed that the topography-limited systems were more vulnerable than recharge-limited systems to SWI and changes in freshwater flow to the sea. In their approach, the variations in recharge rate in combination with only the vertical movement of SLR were modeled.

2.3. Aquifer bed slope impacts on SLR-induced SWI

Coastal aquifer beds which can be inclined toward the sea or toward the land can obviously affect the behavior of SWI. In reality coastal aquifers mostly have inclined beds (Abarca et al., 2007; Koussis et al., 2015). Examples of such unconfined aquifers with inclined bed boundary include the Mediterranean coastal aquifers (Sherif and Singh, 1999; Mazi et al., 2014; Koussis et al., 2015), and the Akrotiri coastal aquifer in Cyprus (Mazi et al., 2014) which were studied in detail by Mazi et al. (2014).

Conceptualizing the beds of coastal aquifers as horizontal has been a common assumption in most previous studies (e.g. Kooi et al., 2000; Werner and Simmons, 2009; Ataie-Ashtiani et al., 2013a, 2014; Chesnaux, 2015; Morgan et al., 2015). This conceptualization does not correspond to reality in general and it serves mainly the purpose of analytical mathematical convenience (Koussis et al., 2012). Abarca et al. (2007) investigated density-dependent flow processes caused by three-dimensional confined aquifer geometry using numerical simulations considering a lateral slope of the aquifer boundaries. They showed the intrusion of seawater is controlled more by this slope than by the aquifer thickness and dispersivity. Koussis et al. (2012) focused for the first time to understand how this conceptualization influences SWI behavior by analytical methods. They extended the analytical Strack (1976) discharge potential solution to steady-state sharp interface flow in unconfined coastal aquifers under both FC and HC LWBCs by approximating the gravity-driven flow component and representing the aquifer geometry in a schematized yet realistic manner.

Using the generalized analytical sharp interface model of Koussis et al. (2012), Mazi et al. (2013) investigated the responses of SWI to SLR in coastal aquifers. They examined the impacts of SLR of 0.59 m and 1.6 m on both FC and HC LWBCs while they ignored the impacts of LSI. The effects of the aquifer bed slopes of −1%, 0%, and 1%, the hydraulic conductivity, and the original sea level on seawater toe location were studied in their work. Their assessments demonstrated the important effect of aquifer bed slope on original seawater toe location and also on its responses to SLR. The aquifer bed slope impact is particularly important under FC LWBCs, for which SLR also raises the aquifer free surface, which increases aquifer transmissivity and therefore enhances SWI (Mazi et al., 2013). Recently, Koussis et al. (2015) studied two regional Mediterranean aquifers with no-flow LWBCs and with HC LWBCs, considering the aquifer bed slope of them. The effects of the aquifer bed slope on the original seawater toe location in these real-world cases were previously explored by Mazi et al. (2014). Koussis et al. (2015) corrected and applied the Koussis et al. (2012) analytical sharp interface solution of SWI. SLR of 1 m without LSI was considered in their study. The important effects of LWBCs and aquifer bed slope on seawater toe location were also shown in their study.

2.4. Overshoot and seawater fingering phenomena due to SLR

Some SLR-induced time-related phenomena such as overshoot mechanism (e.g. Watson et al., 2010; Chang et al., 2011; Morgan et al., 2015) and seawater fingering from land surface into aquifers (e.g. Kooi et al., 2000; Laattoe et al., 2013) have been documented in the literature (see Table 1).

Overshoot means that seawater which intrudes into a coastal aquifer due to SLR would initially overshoot the steady-state position but then naturally be driven back to a seaward resting position (e.g. Chang et al., 2011). For the first time, Watson et al. (2010) focused on to the temporary overshoot caused by SLR. They investigated the transience of SLR-SWI in typical coastal aquifer settings using both analytical and FEFLOW numerical models. The important issue of associated time scales for overshoot phenomena was neglected in Watson et al. (2010). They observed the overshoot of the post SLR steady-state seawater toe location by up to 250% in several of the simulated scenarios. They considered only FC LWBCs in their experiments. Their results indicated greater potential for more rapid toe response, possibly leading to overshoot, for higher values of aquifer specific yield and aquifer length and lower system thickness and hydraulic conductivities. They highlighted that the overshoot phenomenon contradicts the common assumption that steady-state results are the worst for SLR-induced SWI. Watson et al. (2010) assumed an instantaneous SLR of 1 m while the impacts of LSI and aquifer bed slope were ignored in their study. They mentioned that the instantaneous nature of SLR enhances the water table wave generation which can also affect the overshoot mechanism. They predicted that by implementation of an instantaneous SLR, the SWI obtained from numerical modeling is more rapid than would occur due to more realistic gradual SLR.

Chang et al. (2011) performed numerical experiments using SEAWAT to study the transient effects of SLR on SWI in both confined and unconfined FC aquifers. Their results showed the occurrence of overshoot due to SLR in confined aquifers while for unconfined aquifers; this mechanism would have less effect due to changes in the value of the effective transmissivity. A minor impact of land-surface slope on the overshoot mechanism was shown by Morgan et al. (2013) as a part of physical and numerical sand tank experiments with 2.0 m length, 0.5 m height, and 0.05 m width. Their results under a FC unconfined aquifer setting confirmed that the SWI overshoot could be observed under controlled laboratory conditions and the land-surface slope did not control the spatial extent of overshoot. Morgan et al. (2013) showed that the magnitude of overshoot for SLR in the physical experiments was 24% of the change in steady-state seawater toe location. They mentioned that this magnitude was observed under the laboratory setting which was designed to maximize the overshoot extent by adopting the high groundwater flow gradients and large and rapid SLRs. Morgan et al. (2013) predicted that the overshoot at the field scale appears to be low and further investigation should be performed to clarify the associated behaviors.

Recently, Morgan et al. (2015) used numerical modeling of SLR-SWI to assess the occurrence of SWI overshoot within realistic aquifer settings. They aimed to compare both the instantaneous (1 m) and the gradual SLR scenarios (10 mm/yr over 100 years) under both FC and HC LWBCs. Similar to the majority of the previous studies, the impacts of LSI and aquifer bed slope were ignored in their research. As mentioned previously, the gradual SLR assumption is more realistic and near the high end of IPCC (2013) projections. Morgan et al. (2015) described that no significant overshoot was produced in the confined aquifer cases while the overshoot could occur within realistic unconfined aquifer settings with FC LWBCs. Their results are not in agreement with the conclusion of Chang et al. (2011) on this pattern. Their experiments indicated that heads re-equilibrated rapidly and overshoot was not observed on all HC cases. They also showed that the overshoot is possible under gradual SLR conditions, albeit in the fewer number of cases and with lower magnitudes. Their results also confirmed the previous findings that the effects of SLR on the FC aquifers are small. In Morgan et al. (2015) tests, due to the overshoot, the seawater toe locations passed the steady-state location approximately 50 years after SLR started, which were half the 100-years simulated period.

Another time-related phenomenon which was recommended for further investigation by Watson et al. (2010) is the resultant potential for convective seawater fingers due to SLR-induced LSI. Seawater fingering here refers to the plumes of seawater migrating downwards from the land surface due to finger instabilities that result from the unstable nature of the density stratification when seawater resides on top of underlying freshwater and the influence of gravity (Kooi et al., 2000). Transient seawater fingering associated with free convection from the land surface can potentially occur when the land surface is submerged with seawater as a result of SLR (Ataie-Ashtiani et al., 2013a; Laattoe et al., 2013).

Kooi et al. (2000) assessed the SWI caused by the gradual SLR of 1 mm/year and LSI at geological time scales based on the simulated transient seawater fingers occurring under unstable density conditions. They distinguished four modes of SWI by application of numerical experiments. Based on their methodology, Laattoe et al. (2013) extended the analysis of Kooi et al. (2000) to a wider range of land-surface slope, the geological time frames, and the relatively fine-grained sediments under both FC and HC LWBCs. They assessed only cases with horizontal bed boundaries and simulated the temporal behavior of SWI, fluid and salt fluxes across all boundaries, and the total mass of salt in the domain. Laattoe et al. (2013) highlighted that SWI fingers occur only for scenarios which considered LSI effects with larger values of hydraulic conductivity and faster rates of SLR in flatter coasts. They obtained that the rates of SLR-SWI were equivalent in both FC and HC systems when LSI effects were included in the model. Kooi et al. (2000) and Laattoe et al. (2013) are just previous studies considered free convection during SLR and more detailed investigations particularly under real-world conditions are not found in the literature.

In the abovementioned sub-sections, using Table 1 and Figs. 2 and 3 which provide a novel tabulated and diagrammatic condensation of all the previous studies, the analysis of available literatures regarding the impacts of SLR is considered. The main characteristics of those studies can be observed and compared easily using the proposed table and figures. In addition, some remaining main challenges of this field need to be considered to appropriately characterize the key controlling factors. These are briefly described in the following section.

3. Future research challenges

Based on the review, a list of future challenges is identified in this section. All previous studies have investigated a subset of controlling processes without considering many other ones that may be expected to exert a significant control on SWI processes. Integration of all the purported controlling factors studies in previous literature into a single, unifying, framework is required to conduct the fully-integrated analyses. Simultaneously examining many of the controlling factors, within the same analysis framework, remains an active field for future research and will help to continuously improve our understanding of their relative significance.

Ataie-Ashtiani et al. (2013a) briefly listed a number of challenges such as considering topographic slopes, coastal erosion, change in beach morphology, geologic heterogeneities, transition zone of freshwater and seawater, spatial dimensionality, pumping, possible effects of extraction and injection in costal aquifers, intensity and frequency of storm events, wave and tide, and various site-specific effects as important fields for further research. Watson et al. (2010) and Morgan et al. (2015) briefly described the need for further study on scenarios of gradual SLR which are more consistent with climatic driven conditions. Also, comparative investigations under more realistic SLR scenarios, such as those presented by IPCC (2013), have potential opportunities for future research.

An examination of time-related phenomena such as overshoot and seawater fingers with more realistic assumptions such as gradual SLR is another open field. Both of them may be transient behavior of SWI. The time-scale for their occurrence can be an issue for investigation. Seawater fingers can potentially occur when the LSI impact is considered. However, as mentioned by Kooi et al. (2000) in a study of long-time scale impacts on aquifers, the occurrence of seawater fingers may depend on the various modes of SWI that can take place under transient conditions. These various modes require further research in the specific context of the shorter term SLR impacts studied in research.

It is noteworthy that most previous studies in this field considered only hypothetical or highly simplified coastal aquifers. Future research in this field needs to extend, develop, and evaluate the climate change effects in the context of real-world cases, which are usually characterized by large scales, geologic heterogeneity properties, limited data, and a variety of site-specific processes occurring over a range of scales. For example, Stigter et al. (2014) have comparatively assessed the SLR impacts on three coastal aquifers in the Mediterranean using future scenarios for three different parameters of the recharge rate, the crop water demand, and SLR. Mahmoodzadeh et al. (2014) have recently presented such a study for Kish Island in the Persian Gulf, Iran.

One of the missing aspects in calls for further research is incorporating climate change impacts into coastal groundwater management plans and decision-making models, particularly for real-world cases which are actually exposed to such global and significant concerns (Ketabchi and Ataie-Ashtiani, 2015a–c). Ketabchi and Ataie-Ashtiani (2015b) have provided a comprehensive review on coastal groundwater optimization and this need has also emphasized in their review. Recently, for Kish Island in Iran, a parallel evolutionary optimization approach was employed by Ketabchi and Ataie-Ashtiani (2015c) to determine optimal management strategies. In their study, an optimization solution for the case study of a scenario of SLR indicated that a reduction of 20% in groundwater extraction rate was mainly due to LSI which confirmed the significance of the inclusion of SLR impacts in coastal aquifers management problems.

A large number of recent studies considered coastal aquifers, where the freshwater is constrained at the lower boundary by the aquifer bed. But many other coastal aquifers, such as those occurring in small islands, have a very different nature and require additional studies. The limited number of studies of SWI and fresh groundwater resources on small islands such as Terry and Falkland (2010), Ataie-Ashtiani et al. (2013b), Ketabchi et al. (2014), Mahmoodzadeh et al. (2014), and Ketabchi and Ataie-Ashtiani (2015b,c) conceptually assessed such coastal aquifers, considering the impacts of most influential factors. Therefore, further clarification and interpretation is necessary on many aspects pertaining to SWI and fresh groundwater resources on small islands.

There is also an important scope for investigating the practical ways to control and lessen the negative impacts of SWI, to improve the effectiveness of engineering measures to mitigate SLR-induced SWI, and to design monitoring programs for the purpose of data acquisition. The LSI (particularly in flatter coastal regions), is one of the most important factors that can be studied in such efforts. Some key tasks to reduce substantial gaps between the knowledge of climate change and the proposed impacts on SWI and practical strategies are undoubtedly crucial (Werner et al., 2013; Ojha et al., 2015).

Climate change parameters and processes and their impacts on groundwater resources are essentially uncertain. The related challenges result from the inherent challenges in modeling the uncertainties associated with a future climate (Werner et al., 2013; Ojha et al., 2015). Therefore, to address these issues it is often necessary to invoke stochastic approaches. For such investigations, some researchers such as Sreekanth and Datta (2014), Rajabi and Ataie-Ashtiani (2014) and Rajabi et al. (2015b) provided a solution to improve the efficiency of Monte Carlo simulations for uncertainty propagation analysis in SWI numerical models. Rajabi et al. (2015a) proposed the application of non-intrusive polynomial chaos expansion meta-models instead of the original numerical models for uncertainty propagation and global sensitivity analyses. The use of such methodologies are recommended for stochastic assessments and global sensitivity analyses because the less computational time is required for generating the sample designs which are needed to reach a certain level of accuracy.

To address the need to quantitatively examine the combined and relative effects of SLR, associated LSI according to land-surface and aquifer bed slopes, and LWBCs on SWI in unconfined coastal aquifers, we extend the analytical solutions of Koussis et al. (2012, 2015) to sloping aquifers and present those in a dimensionless form. These new solutions can consider LSI impacts in the proposed formulations. Using a framework that includes such known influential controls not only allows us to quantify the relative importance of these controls as well as to make some early progress towards a more generalized understanding of these controls on SWI processes.

In the following, firstly the sensitivity of seawater toe location to various influential factors in sloping aquifers is investigated. The simplicity of the used analytical formulations is an advantage of the method applied, as using the simplest possible mean provides an important and novel insight into the problem of SLR impacts on SWI (Ataie-Ashtiani et al., 2013a). Using these analytical solutions, a sloping coastal aquifer as a base case is focused. Moreover, numerical simulations of SWI are performed to extend the analysis to consider dispersion effects and to demonstrate the transient behaviors of such aquifer systems. The assessments on a base case is as an opening to comprehensive integrated studies and it is still necessary to progressively examine even more factors in an integrated modeling framework using a range of realistic parameters.

4. Integrated assessments using analytical modeling

The main objective in this section is to propose a simple tool for seawater toe location sensitivity assessments that are based on fundamental SWI mathematics as applied to a variety of idealized settings. Here, sensitivity refers to the relative propensity for SWI to occur. The basis of the methodology is that the rates of change in seawater toe location assessments in response to stress changes, described as partial derivatives of equations, offer insight into the propensity for SWI (Werner et al., 2012). This adopted approach for sensitivity assessments is similar to that of Werner et al. (2012), Ketabchi et al. (2014, 2016) and Morgan and Werner (2014).

4.1. Methodology

An unconfined coastal aquifer with an inclined land surface and an impervious inclined aquifer bed boundary is considered as shown in Fig. 4. The aquifer is isotropic and homogeneous. A sharp freshwater-saltwater interface and steady-state conditions are assumed.

Recently, Koussis et al. (2015) presented new analytical solutions to estimate the seawater toe location. In their solutions, the implemented corrections improved the accuracy of one-dimensional Dupuit-Forchheimer models of interface flow by modifying the submarine outflow-gap correction (Van der Veer's, 1977) to also account for the influence of transverse dispersion dependent density-factor (Pool and Carrera, 2011). The original solutions of Koussis et al. (2015) lead in the FC systems to Eq. (1) and in the HC systems to Eq. (2) for the seawater toe location that were adopted from Koussis et al. (2012):

$$\left[\delta(1+\delta)\sin^2\varphi + \frac{W}{K}\right]X_{\mathrm{Toe}}^2 - 2\left[\delta(1+\delta)\sin\varphi h_{\mathrm{SW}} + \frac{Q_f}{K}\right]X_{\mathrm{Toe}} + \delta(1+\delta)h_{\mathrm{SW}}^2 = 0 \tag{1}$$

$$[(1+\delta)\sin^2\varphi]X_{\mathrm{Toe}}^3 + \left[\frac{WL}{K} + \sin\varphi[2h_0 - (1+\delta)(2h_{\mathrm{SW}} - \delta L\sin\varphi)]\right]X_{\mathrm{Toe}}^2 - \left[\frac{WL^2}{K} + h_{\mathrm{LW}}^2 - (1+\delta)h_{\mathrm{SW}}^2 + 2L\sin\varphi[h_0 + \delta(1+\delta)h_{\mathrm{SW}}]\right]X_{\mathrm{Toe}} + L\delta(1+\delta)h_{\mathrm{SW}}^2 = 0 \tag{2}$$

where δ [–] is $(\rho_s - \rho_f)/\rho_f$, ρ_s [M L^{-3}] is the density of seawater, ρ_f [M L^{-3}] is the density of freshwater, φ [–] is the angle of impervious aquifer bed against the horizontal. For Eq. (2), the value of h_0 must be estimated through iteration, for example, by iterating on $h_0 = [h(X_{\mathrm{Toe}}) + h_{\mathrm{SW}}]/2$ where $h(X_{\mathrm{Toe}}) = (1+\delta)(h_{\mathrm{SW}} - X_{\mathrm{Toe}}\sin\varphi)$.

To consider the corrections of submarine outflow gap (Van der Veer's, 1977) and transverse dispersion dependent density factor (Pool and Carrera, 2011), the following modifications can be implemented (Koussis et al., 2015): (1) δ is corrected to δ^c. δ^c is $\delta[1-(\alpha_T/B)^{0.65}]$ where α_T is transverse dispersivity and B is average aquifer thickness which is defined as the depth below the mean sea level to the aquifer bed elevation (see Fig. 4). For aquifers with an inclined bed, the corresponding value for B can be estimated by $h_{\mathrm{SW}} - 0.5L\tan\varphi$; and (2) h_{SW} is corrected to $h_{\mathrm{SW}}^c = h_{\mathrm{SW}} - \xi_0$ where ξ_0 (the depth of the interface below the water table outcrop at the coast) is written as:

$$\xi_0 = \left[\frac{1}{[(W+K\delta^c)/(K\delta^c)]\delta^c(1+\delta^c)}\right]\left[\frac{W\chi_0^2 + 2Q_f\chi_0}{K}\right] \tag{3}$$

where χ_0 (the width of the gap through the submarine outflow) is defined as:

$$\chi_0 = \frac{Q_f\left[1 - \sqrt{1 - \left(\frac{W}{K}\right)\left(\frac{1-(\delta^c+W/K)}{(1-W/K)(\delta^c+W/K)}\right)}\right]}{W\sqrt{1 - \left(\frac{W}{K}\right)\left(\frac{1-(\delta^c+W/K)}{(1-W/K)(\delta^c+W/K)}\right)}} \tag{4}$$

To account for LSI, similar approaches as Ataie-Ashtiani et al. (2013a) and Ketabchi et al. (2014) are considered. A shift in the position of the coastline caused by SLR of Δh_{SW} and thus the LSI of $\Delta h_{\mathrm{SW}}/S$, where S [–] is land-surface slope (as shown in Fig. 4), the new steady-state seawater toe location after SLR is given by replacing h_{SW} with $h_{\mathrm{SW}} + \Delta h_{\mathrm{SW}}$, L with $L - \Delta h_{\mathrm{SW}}/S$, and X_{Toe} with $X_{\mathrm{Toe}} - \Delta h_{\mathrm{SW}}/S$ due to SLR and the associated LSI, for both FC and HC landward boundaries. These changes extend the analytical solutions of Koussis et al. (2012, 2015) to sloping aquifers which can consider the impacts of both SLR and the associated LSI. Therefore, this extension is based on the Dupuit-Forchheimer approximation and we have modified the aquifers length, as suggested by Ataie-Ashtiani et al. (2013a) and Ketabchi et al. (2014), because of the landward movement of the coastline due to SLR. Also, it is assumed that only the top of the outflow section is inclined, so that upon SLR, the inundated coast diminishes the recharge area and the outflow rate while the remaining outflow area is vertical.

Using dimensionless assessments helps to simplify the interpretation of basic phenomena by reducing the number of study parameters and also allows generalization of the results to other cases with different parameters (Ketabchi et al., 2014, 2016). Therefore, the following dimensionless parameters are considered in this study (Ketabchi et al., 2014):

$$W^* = \frac{W}{K} \quad h^* = \frac{h}{L} \quad B^* = \frac{B}{L} \quad X_{\mathrm{Toe}}^* = \frac{X_{\mathrm{Toe}}}{L} \quad Q_f^* = \frac{Q_f}{KL} \quad q_b^* = \frac{q_b}{KL} \tag{5}$$

By replacement of these parameters, the dimensionless forms of Eqs. (1) and (2) are given as:

$$[\delta(1+\delta)\sin^2\varphi + W^*]X_{\mathrm{Toe}}^{*2} - 2[\delta(1+\delta)\sin\varphi h_{\mathrm{SW}}^* + Q_f^*]X_{\mathrm{Toe}}^* + \delta(1+\delta)h_{\mathrm{SW}}^{*2} = 0 \tag{6}$$

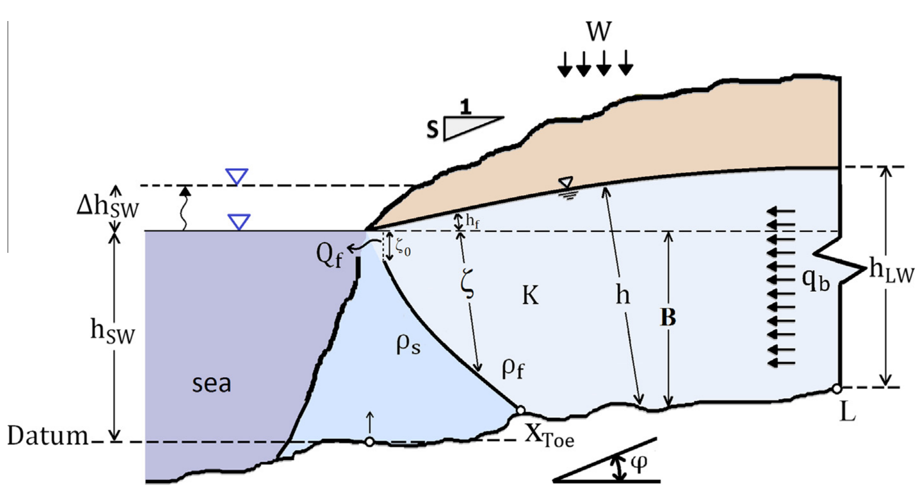

Fig. 4. Schematic of a sloping unconfined coastal aquifer with inclined aquifer bed boundary (used for analytical models).

$$
\begin{aligned}
&[(1+\delta)\sin^2\varphi]X^{*3}_{\mathrm{Toe}} + [W^* + \sin\varphi[2h^*_0 - (1+\delta)(2h^*_{\mathrm{SW}} - \delta sin\varphi)]]X^{*2}_{\mathrm{Toe}} \\
&\quad - [W^* + h^{*2}_{\mathrm{LW}} - (1+\delta)h^{*2}_{\mathrm{SW}} + 2\sin\varphi[h^*_0 + \delta(1+\delta)h^*_{\mathrm{SW}}]]X^*_{\mathrm{Toe}} \\
&\quad + \delta(1+\delta)h^{*2}_{\mathrm{SW}} = 0
\end{aligned} \tag{7}
$$

Moreover, the modifications of Koussis et al. (2015) and the given method here to consider the impacts of SLR and LSI can be applied in the dimensionless Eqs. (6) and (7).

The dimensionless parameters are utilized to carry out the sensitivity assessments. The sensitivity of the seawater toe location to the influential factors of δ, $\sin\varphi$, W^*, Q^*_f, B^*, h^*_{LW}, Δh^*_{SW}, and S can be obtained by differentiating Eqs. (6) and (7) with respect to the proposed factor, which are used for our dimensionless sensitivity assessments using a base case in the next section.

Table 2
Modeling parameters for a base case aquifer.

Symbol	Parameter	Value
L	Aquifer length (m)	1000
φ	Aquifer bed slopes (%)	0 and 1
S	Land-surface slopes (%)	0.5 and 5
h_{SW}	Mean sea level (m)	30
ρ_f	Freshwater density (kg/m^3)	1000
ρ_s	Seawater density (kg/m^3)	1025
C_f	Freshwater concentration (kg/ m^3)	0
C_s	Seawater concentration (kg/m^3)	35
W	Recharge rate (mm/year)	18.25
q_b	Regional flux rate (m^2/day)	0.15
μ	Fluid dynamic viscosity (kg/m.s)	0.001
D_m	Molecular diffusion (m^2/s)	1.48×10^{-9}
g	Gravitational acceleration (m/s^2)	9.81
ε	Effective porosity (–)	0.20
K	Hydraulic conductivity (m/day)	10
S_s	Specific storage (1/m)	0.008
α_L	Longitudinal dispersivity (m)	1
α_T	Transverse dispersivity (m)	0.1

4.2. Sensitivity assessments

The present analytical solution gives a convenient tool to investigate and to integrate the influence of parameters in a wide range without the possible computational demands for numerical simulations. The considered coastal aquifer as a base case here is modified from Chang et al. (2011) conceptual model. The hydrogeologic parameters are chosen to be similar to a case studied by Chang et al. (2011) although other equally appropriate base cases could be chosen. They derived their hydrogeologic parameters from the SWI field's investigation in the Pioneer Valley, Australia (Werner and Gallagher, 2006). This framework allows us to analyze the effects of the land-surface and aquifer bed slopes and climatic factors on seawater toe location.

Table 2 lists the modeling parameters used for all experiments conducted on a base case. Parameters considered are in the range of typical parameters employed by previous investigations. Land-surface slope values of 0.5% and 5% have been chosen based on previous studies (e.g. Wheater et al., 2010; Laattoe et al., 2013; Ataie-Ashtiani et al., 2013a; Ketabchi et al., 2014). Aquifer bed slopes of 0% (horizontal impermeable aquifer bed) and 1% are also adopted based on Mazi et al. (2013) and Koussis et al. (2015).

Table 3 summarizes the sensitivity assessments of seawater toe location changes (X^*_{Toe}) to the influential factors, under the SLR scenarios with and without the LSI. SLR impacts with and without LSI are one of the main focuses of this assessment. The results are only presented for a case with the land-surface slope of 0.5% and the 1% aquifer bed slope. Such assessments are similar to the analyses of Werner et al. (2012) and Morgan and Werner (2014) on SWI vulnerability indicators. In Table 3, the trend values are obtained on the basis of linear relationships between absolute sensitivity values of the proposed parameters and the proposed values of SLR for both FC and HC LWBCs. The positive trends confirm that SLR intensifies the impacts of the considered factor on X^*_{Toe}, and without LSI effects, these impacts in this illustration is different for a variety of conditions. In addition, the negative trends represent the inverse relation between the dimensionless sensitivity values

Table 3
Sensitivity assessment of the dimensionless seawater toe location.

Sensitivities[a]	LSI	FC						HC					
		SLR (m)						SLR (m)					
		0	0.25	0.5	0.75	1	Trend[b]	0	0.25	0.5	0.75	1	Trend[b]
$\frac{\partial X^*_{\mathrm{Toe}}}{\partial W^*}(-)$	Yes	−14,179.3	−13,656.5	−13,074.6	−12,429.4	−11,716.2	−2461.3	−1729.4	−2010.3	−2354.6	−2688.2	−2664.2	1019.0
	No	−14,179.3	−14,325.2	−14,470.3	−14,614.5	−14,757.7	578.42	−1729.4	−2203.7	−2887.4	−3905.3	−5423.8	3636.1
$\frac{\partial X^*_{\mathrm{Toe}}}{\partial B^*}(-)$	Yes	26.92	27.37	27.83	28.30	28.78	1.86	129.19	178.97	260.98	395.84	542.79	417.63
	No	26.92	27.10	27.28	27.45	27.63	0.708	129.19	172.94	244.87	378.91	658.93	506.18
$\frac{\partial X^*_{\mathrm{Toe}}}{\partial Q^*_f}(-)$[c]	Yes	−18,224.1	−18,905.5	−19,616.5	−20,358.7	−21,134.0	2909.2	−3371.3	−4119.0	−5089.7	−6165.8	−6544.4	3357.2
	No	−18,224.1	−18,491.8	−18,761.3	−19,032.6	−19,305.8	1081.7	−3371.3	−4289.6	−5671.6	−7593.6	−10,578.5	7087.3
$\frac{\partial X^*_{\mathrm{Toe}}}{\partial h^*_{\mathrm{LW}}}(-)$	Yes	–	–	–	–	–	–	−116.29	−160.71	−232.58	−351.57	−535.50	411.71
	No	–	–	–	–	–	–	−116.29	−154.74	−215.91	−322.65	−538.44	404.88
$\frac{\partial X^*_{\mathrm{Toe}}}{\partial \delta}(-)$	Yes	14.12	14.44	14.76	15.08	15.41	1.29	9.39	10.90	12.94	15.63	18.72	9.35
	No	14.12	14.32	14.52	14.71	14.91	0.785	9.39	10.97	13.15	16.33	21.43	11.78
$\frac{\partial X^*_{\mathrm{Toe}}}{\partial \sin\varphi}(-)$	Yes	−11.94	−12.45	−12.98	−13.54	−14.13	2.19	0.449	2.05	4.25	6.80	7.41	7.47
	No	−11.94	−12.20	−12.46	−12.73	−13.01	1.07	0.449	−0.156	−1.26	−3.42	−8.15	8.18
$\frac{\partial X^*_{\mathrm{Toe}}}{\partial \Delta h^*_{\mathrm{SW}}}(-)$	Yes	–	246.27	247.44	248.65	249.91	4.68	–	359.25	426.36	534.03	693.38	368.37
	No	–	27.10	27.28	27.45	27.63	0.695	–	162.08	223.25	327.81	530.95	390.03
$\frac{\partial X^*_{\mathrm{Toe}}}{\partial S}(-)$	Yes	0	−11.02	−22.12	−33.29	−44.55	44.54	0	−9.66	−18.93	−27.00	−31.05	31.78
	No	0	0	0	0	0	0	0	0	0	0	0	0

[a] Based on the dimensionless parameters of $W^* = 5 \times 10^{-6}$, $B^* \approx 0.025 - 0.027$, $Q^*_f \approx 2 \times 10^{-5}$, $h^*_{\mathrm{LW}} = 0.022 - 0.024$, $\delta = 0.025$, $\sin\varphi = 0.01$, $\Delta h^*_{\mathrm{SW}} = 0 - 0.001$, $S = 0.005$ (based on the parameters listed in Table 2).

[b] Trend values obtained based on linear relationship between absolute sensitivities and SLR values.

[c] Q^*_f is given by $(q^*_b + W^*)$ for the FC cases and is estimated by $(W^* \times L^*_{div})$ for the HC cases, where $L^*_{div} = L_{div}/L$ is the dimensionless hydraulic divide location for the HC systems (Koussis et al., 2012; Mazi et al., 2013, 2014).

and SLR i.e. increasing SLR reduces the influence of the factor on X^*_{Toe} (Ketabchi et al., 2014).

Sensitivity of X^*_{Toe} associated with SLR ($\partial X^*_{\mathrm{Toe}}/\partial \Delta h^*_{\mathrm{SW}}$) is higher for the HC cases compared to the FC ones, where the opposite is true for the dimensionless recharge rate variations ($\partial X^*_{\mathrm{Toe}}/\partial W^*$). Similar results were obtained by Werner and Simmons (2009), Werner et al. (2012), Carretero et al. (2013), and Michael et al. (2013). $\partial X^*_{\mathrm{Toe}}/\partial W^*$ is the largest under FC LWBCs which is agreement with the observations of e.g. Werner and Simmons (2009) and Carretero et al. (2013). However, we found that the impacts of W^* cannot be ignored in the HC sloping cases with an inclined aquifer bed. This finding is not in agreement with previous results obtained for HC cases since the influence of land-surface and aquifer bed slopes have been ignored. These results indicate that the LWBCs are important factors in the ranking of coastal aquifer sensitivity to SLR and recharge rate variations. For the FC cases, $\partial X^*_{\mathrm{Toe}}/\partial W^*$ is −14,179.3 under no SLR condition while this sensitivity is reduced to −11,716.2 for a case with 1 m SLR. The trend value of −2461.3 refers to this observation. However, the opposite condition is observed for the HC systems. Sensitivity values for SLR under both FC and HC LWBCs are generally larger when LSI impacts are considered.

As Mazi et al. (2013) showed, the impacts of aquifer thickness i.e. $\partial X^*_{\mathrm{Toe}}/\partial B^*$ are higher in the HC cases. Sensitivity values of the dimensionless thickness (see Table 3) indicate that X^*_{Toe} is less sensitive to B^* changes in the FC aquifer thickness in comparison with those in the HC ones. For all LWBCs (Table 3), Q^*_f has the largest impact on X^*_{Toe} and increasing this factor causes X^*_{Toe} to become smaller, which confirms the previous results of Mazi et al. (2013, 2014). We have shown that both SLR and LSI intensify this impact. Similar behavior is observed under HC LWBCs for h^*_{LW}. δ can also affect X^*_{Toe} but it is negligibly influenced from SLR and LSI. The higher the δ is, the higher X^*_{Toe} is.

The aquifer bed slope impact on X^*_{Toe} is higher for the FC cases as the water table can rise in response to SLR which leads to increase of aquifer transmissivity and consequently X^*_{Toe} (Mazi et al., 2013). SLR impacts increases with increasing aquifer bed slope under both LSI and no LSI considerations at the rate of 2.19 and 1.07 (for the FC cases) and 7.47 and 8.18 (for the HC cases), respectively. This observation indicates that SLR further intensifies the aquifer bed slope impacts on X^*_{Toe} in the HC cases in comparison with those under FC LWBCs. These new insights are gained because of the possibility of integration and combination of SLR, LSI, aquifer bed slope, and LWBCs effects.

The aquifer bed slope impacts was also highlighted by Mazi et al. (2013, 2014) and Koussis et al. (2012, 2015) but they did not focus to such comparative investigations particularly from the aspect of SLR and LSI impacts. As expected, larger LSI and therefore higher X^*_{Toe} are obtained because of a flatter land-surface slope (S), confirming Ataie-Ashtiani et al. (2013a) findings for coastal aquifers and also Ketabchi et al. (2014) and Morgan and Werner (2014) results for island aquifers. The impact of S is significant in both LWBCs although the impact of S is not observed in no LSI consideration. As showed by Ataie-Ashtiani et al. (2013a), this impact is greater in the FC cases compared to the cases under HC LWBCs. For HC LWBCs, vertical movement of sea level has major impacts on X^*_{Toe} (see the sensitivity values of the no LSI cases under HC LWBCs in Table 3) in comparison with the FC cases. However, the FC cases achieve minor influences from only vertical SLR which indicate that the major part of SLR impacts on the FC cases is due to LSI accompanying SLR (compare the sensitivity values of LSI and no LSI cases under FC LWBCs in Table 3).

To further generalize the results to aquifers with wider ranges of lengths and thicknesses the changes of seawater toe location, $\Delta X^*_{\mathrm{Toe}}$, versus B^*, the ratio of the aquifer thickness to the aquifer length, are assessed under SLR of 1 m for both FC and HC cases and the results are shown in Fig. 5. The aquifer length of 1000 m, 10,000 m, and 100,000 m are considered. The aquifer bed slope of 0% and 1% and LSI impacts are also included in Fig. 5.

As can be seen from Fig. 5, $\Delta X^*_{\mathrm{Toe}}$ is more influence by SLR-LSI in deeper aquifers (larger B^*) while for shallower aquifers the SLR-LSI impacts are almost diminished. Larger $\Delta X^*_{\mathrm{Toe}}$ are observed for larger B^* under both FC and HC systems. Similar to Mazi et al. (2013), Table 3 also confirms the higher sensitivity of X^*_{Toe} to B^* in the HC cases compared to FC ones. The illustrated curves in Fig. 5 terminate at maximum $\Delta X^*_{\mathrm{Toe}}$ which occurred at maximum B^*. Mazi et al. (2013) found that maximum $\Delta X^*_{\mathrm{Toe}}$ are imminent at the aquifer thickness with highly nonlinear dependency. As indicated in Fig. 5, LSI intensifies the impacts of SLR under the various considered LWBCs, aquifer dimensions, and aquifer bed slope. Most importantly, aquifer length has an insignificant impact on $\Delta X^*_{\mathrm{Toe}}$ due to SLR-LSI. For example, for FC LWBC and inclined aquifer bed conditions, when B^* of 0.02 is assumed, the values of $\Delta X^*_{\mathrm{Toe}}$ with LSI for 1000 m, 10,000 m, and 100,000 m length of aquifer are 0.2404, 0.0239, and 0.0024 (equivalent to ΔX_{Toe} of 240.4 m, 238.7 m, and 238.6, respectively). Similar behaviors are also observed for the HC cases. In addition, generally considering the influences of aquifer bed slope leads to slightly reduce the impacts on the seawater toe location under various lengths and B^* (compare Fig. 5a and b).

The sensitivity parameters of two real-world coastal aquifers are calculated at the Mediterranean coast (case 1 and case 2) based on the specified modeling parameters summarized in Table 4 (Koussis et al., 2015). The results are summarized in Table 5. The Mediterranean aquifer case 1 has no-flow LWBC. The LWBC of the Mediterranean aquifer case 2 is HC at landward boundary while the associated constant head elevation is assumed to be 11 m above mean sea level.

$\Delta X^*_{\mathrm{Toe}}$ of the Mediterranean aquifer case 1 with B^* of 0.008 is estimated to be 0.022 and 0.00077 with and without LSI, respectively while $\Delta X^*_{\mathrm{Toe}}$ for the base cases with B^* of 0.03 are 0.247 and 0.027, respectively. The dimensionless number of $\Delta X^*_{\mathrm{Toe}}/B^*$ can be used as an indicator for the intensity of aquifer response to the variations. For instance, $\Delta X^*_{\mathrm{Toe}}/B^*$ of 2.8 and 0.096 is estimated for the Mediterranean aquifer case 1 while for the FC base case the values of 8.2 and 0.9 is found with and without LSI, respectively. $\Delta X^*_{\mathrm{Toe}}$ of the Mediterranean aquifer case 2 with B^* of 0.004 is estimated to be 0.237 and 0.064 with and without LSI, respectively. For the HC base case, this value is more than 0.5. $\Delta X^*_{\mathrm{Toe}}/B^*$ of 59.3 and 16.0 is estimated for the Mediterranean aquifer case 2 with and without LSI, respectively while for the HC base case, the values larger than 16 are obtained. The larger values of $\Delta X^*_{\mathrm{Toe}}/B^*$ are observed for the HC cases comparing to the FC cases and for the cases with LSI comparing to the cases with only vertical SLR impacts. These results of these two cases confirm the findings of Fig. 5 for different set of aquifer parameters. Generally, the prominence of considering LSI in all these cases is incontrovertible.

The relative impacts of influential parameters on $\Delta X^*_{\mathrm{Toe}}$ are integrated in Fig. 6 in the investigated cases under SLR of 1. It shows the dominant parameters controlling X^*_{Toe} are Q^*_f and W^*, followed next by with an about an OoM smaller is Δh^*_{SW} for both cases of FC and HC. It is important to note that the main contributors to fresh groundwater discharge to sea are the regional freshwater flux at the landward boundary of FC systems and the groundwater hydraulic gradient for HC systems. For FC LWBCs, the Δh^*_{SW} impact is up to an OoM larger when the LSI impact is considered and generally it has less impact for the HC systems. The B^* influence for the HC cases is significantly larger (an OoM) in comparison with that for the FC cases. The h^*_{LW} impact for the HC cases in Fig. 6 shows that the impact on $\Delta X^*_{\mathrm{Toe}}$ is at the same OoM of the impact of B^*.

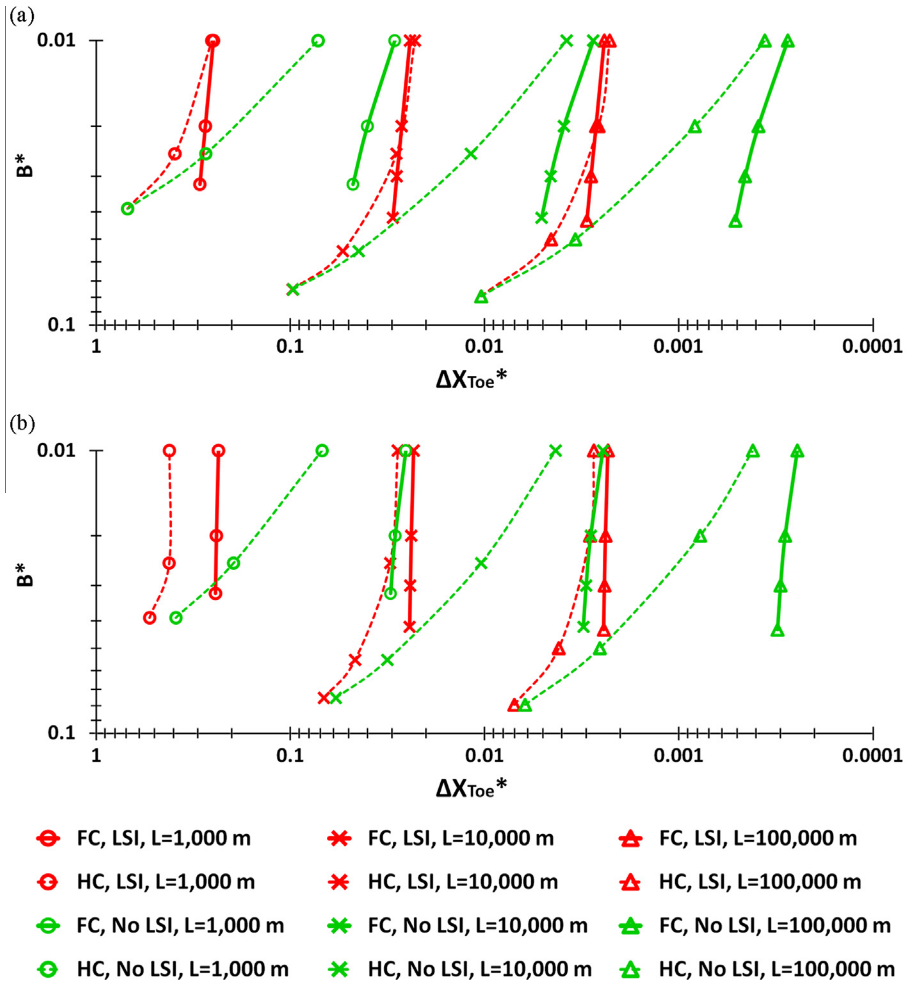

Fig. 5. Impacts of aquifer dimensions on ΔX^*_{Toe} for the FC (solid lines) and the HC (dashed lines) systems: (a) aquifer bed slope of 0%, and (b) aquifer bed slope of 1% (results are shown based on similar modeling parameters of the base case under SLR of 1 m with and without LSI).

Table 4
Modeling parameters for two Mediterranean coastal aquifers.

Symbol	Parameter[a]	Mediterranean coastal aquifers	
		Case 1 (FC)	Case 2 (HC)
L	Aquifer length (m)	20,000	150,000
φ	Aquifer bed slope (%)	1	0.3
S	Land-surface slope (%)	0.25[b]	0.003[c]
h_{SW}	Mean sea level (m)	250	800
ρ_f	Freshwater density (kg/m^3)	1000	1000
ρ_s	Seawater density (kg/m^3)	1025	1025
W	Recharge rate (mm/year)	200	11.85
K	Hydraulic conductivity (m/day)	30	100
α_T	Transverse dispersivity (m)	1	2

[a] The values are adopted from Koussis et al. (2015).
[b] The value is adopted from Yechieli et al. (2010).
[c] The value is estimated from Sefelnasr and Sherif (2014).

The lowest sensitivities are found for δ and $\sin\varphi$ in both FC and HC cases. Although, the assessments demonstrate that the inclusion of land-surface and aquifer bed slopes in SWI investigations is important in both LWBCs as the consideration of horizontal-bed aquifer and ignoring the land-surface slope is markedly simplistic in many cases. The general behaviors and tendencies illustrated in Fig. 6 are almost identical for the cases with similar LWBCs. These observations plausibly establish and generalize the abovementioned results to a variety of extensive ranges of aquifer parameters and characteristics.

Table 5
Sensitivity assessment of the dimensionless seawater toe location for two Mediterranean coastal aquifers.

Sensitivities	LSI	Mediterranean coastal aquifers	
		Case 1 (FC)	Case 2 (HC)
$\frac{\partial X^*_{\text{Toe}}}{\partial W^*}(-)$	Yes	−4915.0	6258.5
	No	−4828.4	−332,916.0
$\frac{\partial X^*_{\text{Toe}}}{\partial B^*}(-)$	Yes	15.55	2464.2
	No	15.23	11,358.0
$\frac{\partial X^*_{\text{Toe}}}{\partial Q^*_f}(-)$[a]	Yes	−5033.4	16,088.9
	No	−4828.4	−675,358.2
$\frac{\partial X^*_{\text{Toe}}}{\partial h^*_{\text{LW}}}(-)$	Yes	–	−2400.0
	No	–	−10,882.8
$\frac{\partial X^*_{\text{Toe}}}{\partial \delta}(-)$	Yes	3.68	6.98
	No	3.61	34.32
$\frac{\partial X^*_{\text{Toe}}}{\partial \sin\varphi}(-)$	Yes	−1.56	−65.48
	No	−1.51	−374.66
$\frac{\partial X^*_{\text{Toe}}}{\partial \Delta h^*_{\text{SW}}}(-)$	Yes	454.21	6220.1
	No	15.30	11,292.7
$\frac{\partial X^*_{\text{Toe}}}{\partial S}(-)$	Yes	−8.77	−0.84
	No	0	0

[a] Q^*_f is given by $(q^*_b + W^*)$ for the FC cases and is estimated by $(W^* \times L^*_{div})$ for the HC cases (Koussis et al., 2012; Mazi et al., 2013, 2014).

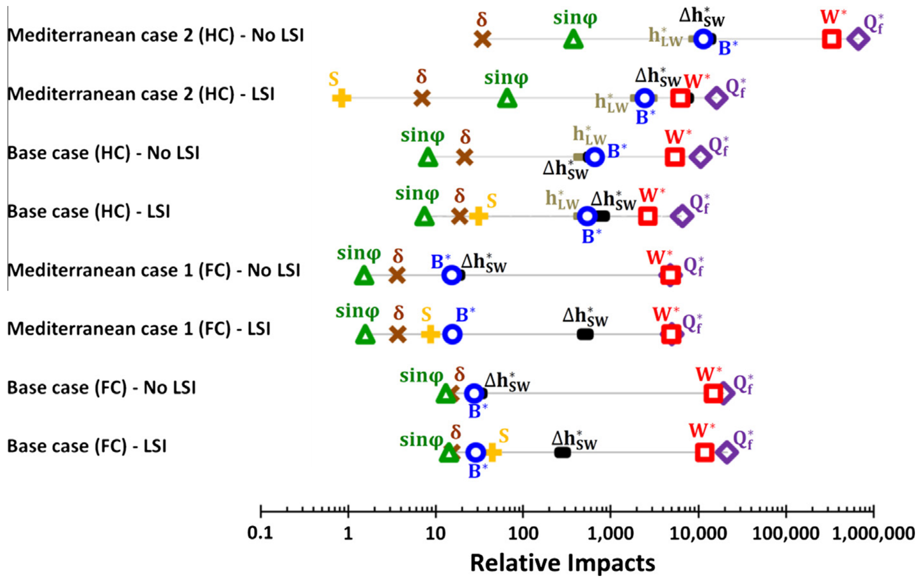

Fig. 6. Summary of relative impacts of influential parameters on ΔX^{*}_{Toe} in the investigated cases under SLR of 1.

To complete the integration purpose of this work, the dispersive and transient behavior of SWI interface will also be addressed in the following section.

5. Integrated assessments using numerical modeling

In this section, the saturated-unsaturated density-dependent flow and transport USGS code SUTRA (Voss and Provost, 2010) is employed. SUTRA (Voss and Provost, 2010) has been previously used by e.g. Michael et al. (2013), Ketabchi et al. (2014), Mahmoodzadeh et al. (2014), and Ketabchi and Ataie-Ashtiani (2015c) for investigating the SLR-induced SWI in coastal aquifers.

Schematized unconfined aquifer cross-sections (based on the presented data in Table 2) used for modeling with finite-element mesh and assigned boundary conditions are illustrated in Fig. 7. These cases are similar to the base case assessed in the previous section under both FC and HC LWBCs. In line with all previous studies, some of the secondary factors such as the impacts of tidal fluctuations and waves are not considered at the seaward boundary. The numerical model discretization consists of a mesh of 38,544 quadrilateral finite elements (39,071 nodes) for aquifer cross-sections. The mesh is refined near the top and near the seaward boundaries of the domain where a steeper change of hydraulic heads and salinity concentrations are expected. The horizontal size of the mesh, which has 1000 m length, changes from 1 m in

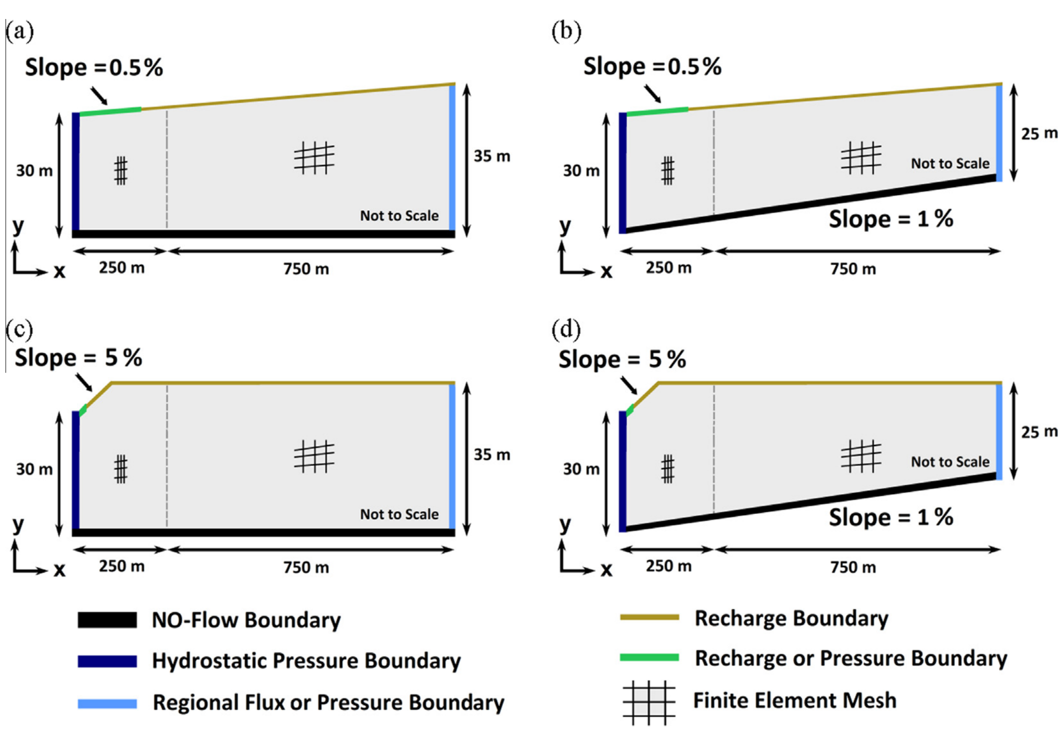

Fig. 7. Geometry of modeling domain of a base case; including boundary conditions with the land-surface slopes of 0.5% and 5%, and the aquifer bed slopes of 0% and 1% (used for numerical models).

the zone near the sea boundaries to 4 m in other parts. Also, the mesh size has varying lengths of 0.15–0.57 m in the vertical direction. Following testing of various finer and coarser discretization schemes in the range of 9636–618,809 nodes, the abovementioned discretization is adopted. The results of the mesh size test show an appropriate level of grid convergence, where the numerical solutions no longer change substantially as a function of grid size. The applied discretization also satisfies the spatial stability criterion (i.e. the grid Peclet number is smaller than four) (Voss and Souza, 1987; Voss and Provost, 2010).

We have assessed a few scenarios here while such assessments can be extended to a variety of influential parameters. In these numerical assessments, instantaneous SLR, similar to the approach adopted by Watson et al. (2010), Chang et al. (2011), Sefelnasr and Sherif (2014), Michael et al. (2013), Ataie-Ashtiani et al. (2013a), Mazi et al. (2013), Ketabchi et al. (2014), and Mahmoodzadeh et al. (2014), is considered. SLR of 1 m condition is considered in the adopted scenarios, based on maximum IPCC (2013) predictions with LSI.

In the present numerical analyses, realistic topographic slopes are simplified to a constant land-surface slope of coastal aquifer (0.5% and 5%). This simplification is similar to the concept applied by previous authors e.g. Abarca et al. (2007), Koussis et al. (2012, 2015), and Ataie-Ashtiani et al. (2013a). Furthermore, based on the similar simplification, the impervious aquifer bed slopes of 0% and 1% are considered (see Fig. 7).

To achieve the equivalent base case configurations for both FC and HC systems, the applied hydraulic head at the landward boundary prior to the SLR is determined from the calculated head at the inland boundary in the corresponding FC LWBCs simulation. This makes the same initial SWI conditions for both LWBCs as the original steady-state equilibrium of the SWI position (Mazi et al., 2013; Morgan et al., 2015). In each scenario, the total simulation time period is set equal to 500 years. The time step size is initially set equal to 500 s and successively increases by a time step multiplier of 1.2 within a 10 time step cycle until it reaches a maximum allowed time step of 90 h. The temporal discretization chosen ensures that the velocities and spatial discretization maintain the Courant number to be less than 0.75 (Voss and Souza, 1987; Voss and Provost, 2010).

The water table position for both LWBCs is shown in Fig. 8 and 100 years after SLR of 1 m and for the land-surface slopes of 0.5% and 5%. For the FC systems and under both land-surface slopes of 0.5% and 5%, the initial hydraulic head at the landward boundary prior to SLR is about 31 m. When the sea-level is raised instantaneously from 30 m to 31 m, the freshwater level at the landward boundary reaches a magnitude of about 32 m to 32.5 m. It is almost the same as the SLR forcing at the seaward hydraulic head. Under the HC systems, the hydraulic head at the landward boundary prior to the SLR remains constant after SLR. Such systems experience a reduction in fresh groundwater discharge to the sea and SWI enhancement relative to the FC systems due to a reduced hydraulic gradient (Michael et al., 2013).

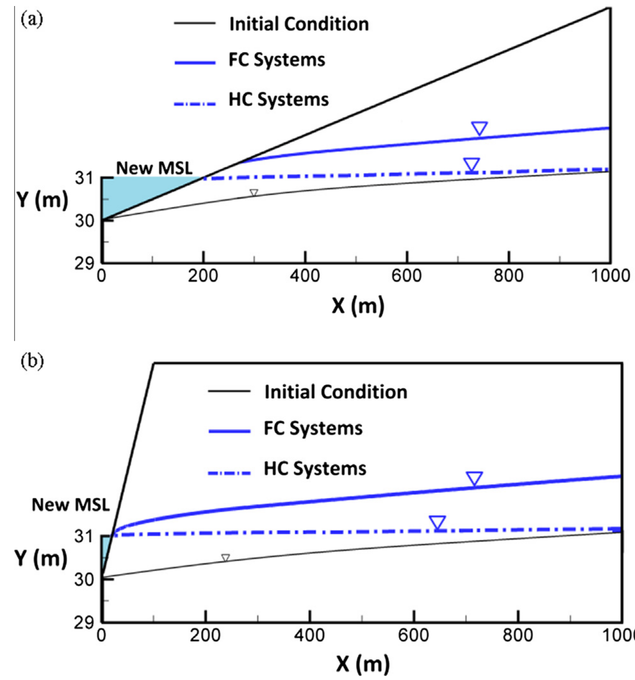

Fig. 8. The water table position, 100 years after SLR of 1 m and for the FC (solid lines) and the HC (dashed lines) systems: (a) the land-surface slope of 0.5%, and (b) the land-surface slope of 5%.

5.1. Sensitivity assessments

A combined comparison of the effects of all considered influential factors on SWI is provided in this section. The percentage values of $\Delta X^*_{\mathrm{Toe}}$ are calculated based on the initial seawater toe location. The results obtained from this comparison are discussed in the following using X^*_{Toe} and dimensionless time ($t^* = tKB/\varepsilon L^2$), where ε [–] is the effective porosity and t [T] is time. The dimensionless time definition has been previously applied e.g. by Watson et al. (2010) and Morgan et al. (2015). The seawater toe location changes have been widely considered in the earlier SLR-related works such as Watson et al. (2010), Ataie-Ashtiani et al. (2013a), and Mazi et al. (2013) to indicate the sensitivity of SWI to the impacts of controlling factors.

It is worth mentioning that a detailed examination of Figs. 2 and 3 shows that our parameterization and results are comparable with the several real-world coastal aquifers and hypothetical ones that have employed realistic parameters. This provides a more general interpretation based on the findings of the present study. A comparison of the role of LWBCs under different conditions such as various land-surface and aquifer bed slopes and the associated LSI are considered in the following using the numerical simulations and the associated assessments are given.

5.1.1. Impacts of SLR and LSI

Fig. 9 shows the salinity distribution of SWI for the cases considered in numerical assessments. In this figure, solid lines indicate the 50% seawater interface. Dashed lines show the 50% seawater interface of the initial steady-state salinity distributions. In all horizontal and inclined aquifer bed simulations, the initial seawater toe locations reach about 409 m ($X^*_{\mathrm{Toe}} = 0.409$) and 340 m ($X^*_{\mathrm{Toe}} = 0.34$), respectively. The results are for 100 years ($t^* = 54.75$) after a SLR of 1 m, while the recharge rate condition is held constant.

Under FC LWBCs, considering SLR without LSI in both land-surface slopes, this seawater toe location reaches about 500 m ($X^*_{\mathrm{Toe}} = 0.5$) and 400 m ($X^*_{\mathrm{Toe}} = 0.4$) from the coastline for the horizontal and the inclined aquifer bed cases, respectively. The results of the FC cases with horizontal aquifer bed slope show that X^*_{Toe} is 0.628 when S is 0.5% and 0.525 for S of 5%, indicating an increase of 53% and 28% compared to the initial seawater toe location, respectively. This difference confirms the significant impact of LSI on SWI. Therefore, the strongest effects on X^*_{Toe} are experienced under the lower land-surface slope due to more inundated lands near the sea and this confirms the results of our analytical assessments and also previous findings (e.g. Melloul and Collin, 2006; Yechieli

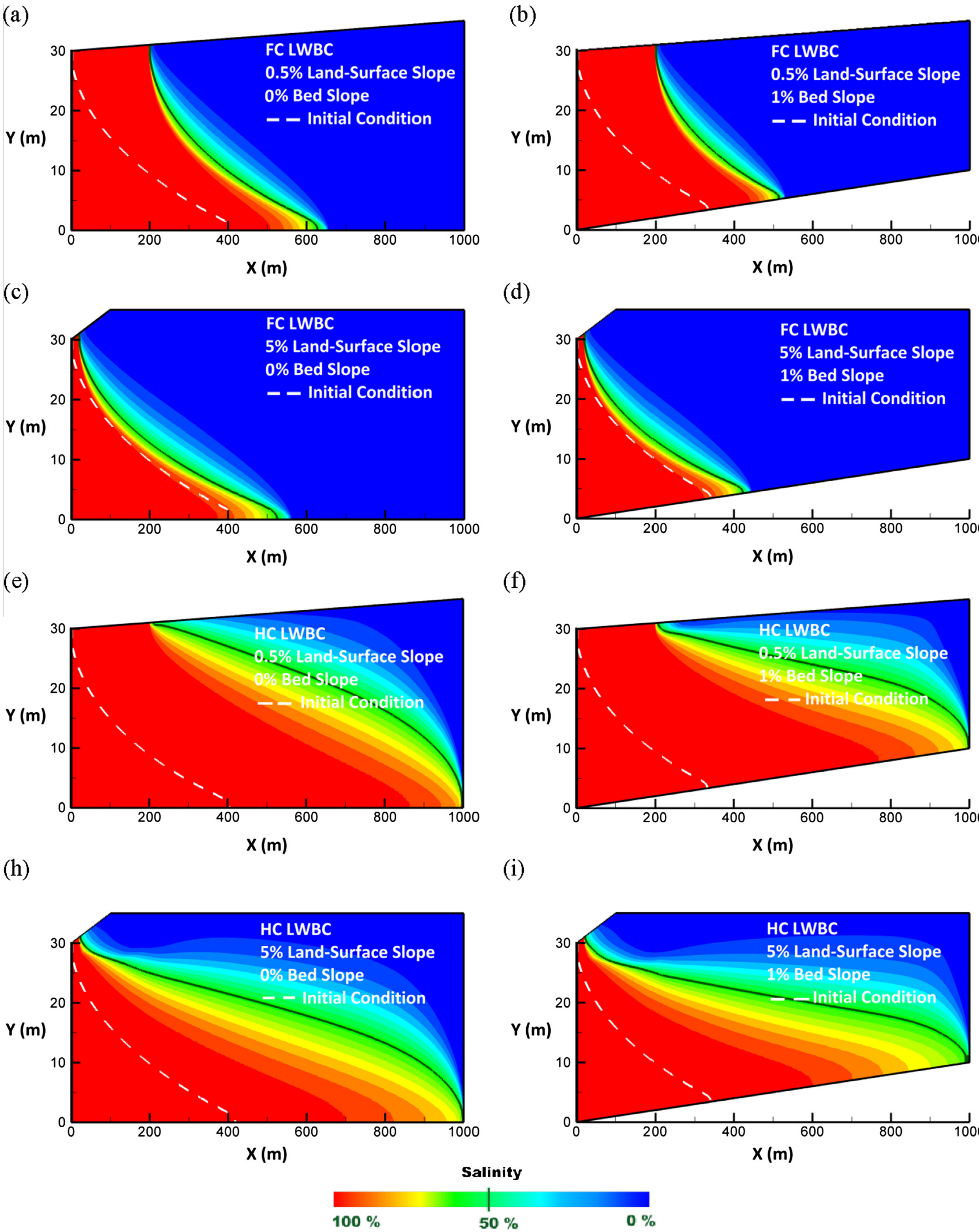

Fig. 9. The salinity distributions, 100 years after a SLR of 1 m based on the numerical simulations (solid black line shows the 50% seawater interface).

et al., 2010; Ataie-Ashtiani et al., 2013a). Similar observations are seen for the cases with 1% aquifer bed slope. The detailed analyses are summarized in Table 6.

Fig. 9 and Table 6 also highlight that the HC cases are associated with significant SWI as a result of SLR in comparison to the FC systems. While for the FC cases, X^{*}_{Toe} is increased between 25% and

Table 6
The comparison of the numerical simulation results under both FC and HC LWBCs ($t^* = 54.75$).

LWBCs	Land-surface slope (%)	Aquifer bed slope (%)	X^*_{Toe}	Difference[a] (%)
FC	0.5	0	0.628	54
FC	0.5	1	0.52	53
FC	5	0	0.525	28
FC	5	1	0.425	25
HC	0.5	0	~1	~144
HC	0.5	1	~1	~194
HC	5	0	~1	~144
HC	5	1	0.995	193

[a] The percentage values are obtained based on the initial seawater toe location.

54% (compared to initial value), under the exact same condition with HC LWBCs, X^*_{Toe} is increased by more than 144% in all cases. These results support the conclusions of our analytical results and also Werner and Simmons (2009), Ataie-Ashtiani et al. (2013a), Mazi et al. (2013), and Carretero et al. (2013) who consistently observed that the HC systems produce larger SWI responses to SLR than FC systems.

As illustrated in Fig. 9 and Table 6, although the SWI response to SLR is less in the FC cases than in the HC ones, impacts due to LSI in both cases cannot be ignored, especially in the flatter coast situations. This new finding is significantly different to previous studies. Laattoe et al. (2013) considered LSI impacts under the limited range of land-surface slopes and obtained results that did not concur with previous studies of Werner and Simmons (2009) and Carretero et al. (2013) who did not considered LSI. The observations of the present study contradict with Laattoe et al. (2013) conclusion which that emphasized the minor differences between the SLR-LSI-induced SWI under both FC and HC LWBCs. In our tests, such condition has not completely been observed and the different hydraulic gradients have been established which cause to different SWI positions (see Table 6).

The comparison of ΔX^*_{Toe} predicted on the basis of both the numerical simulation and the analytical solutions is summarized in Table 7. R values in this table are calculated for our cases in the same way as introduced by Ataie-Ashtiani et al. (2013a). Under the worst conditions with S of 0.5%, R is 1.4 for the horizontal aquifer bed and 3.0 for the inclined aquifer bed under FC LWBCs. Analytical solutions considered in Table 7 demonstrate the larger values of R (larger than 5 and 8) for the abovementioned cases. Therefore, the obtained results indicate that LSI has a significant impact on the SLR-induced SWI but its impacts are less than the magnitudes obtained based on analytical solutions (see Table 6) and emphasized by e.g. Ataie-Ashtiani et al. (2013a). The differences between the predicted ΔX^*_{Toe} by the numerical simulation and the analytical solutions also confirm this fact that in the cases with the flatter coasts, i.e. the larger LSI impacts, ΔX^*_{Toe} are overestimated by the analytical solutions while it is opposite true for the cases with a larger land-surface slope.

The magnitude of X^*_{Toe} by all the analytical solutions is overestimated in comparison with the results of numerical simulations. For example, for the FC case with 0.5% land-surface slope and 1% aquifer bed slope, the initial X^*_{Toe} is estimated to be 0.340 while it reaches 0.520 after a SLR of 1 m. Based on the extension of Koussis et al. (2012) analytical solution, the prior and the post X^*_{Toe} of 0.443 and 0.691 are calculated for this case, respectively. These values are improved to 0.413 and 0.659 using the extension of the corrected analytical formulae of Koussis et al. (2015). It is clear that for this case, both analytical results are overestimated comparing to the results of the numerical simulations. Table 7 shows that the analytical solutions is imprecise in the estimation of the locations of SWI toe under HC LWBCs, whereby the interface moves landward and a steady-state condition cannot be reached.

5.1.2. Overshoot of SWI due to SLR

Fig. 10 depicts the transient seawater toe location and overshoot mechanism behavior associated with a SLR of 1 m for all FC cases. The detailed assessments are summarized in Table 8. For the higher land-surface and the aquifer bed slopes, the total time required to reach a maximum seawater toe location is small. As seen in Table 8, the corresponding t^* taken to reach the maximum values is between 110 and 192 (i.e. 200 years and 400 years for our base case). When we compare the maximum values of the predicted X^*_{Toe} with the values of steady-state seawater toe location, the lower than 2% reversal effect associated with the overshoot mechanism is seen. The hundred year timescale of overshoot occurrence and the associated negligible impact on X^*_{Toe} suggest that the overshoot mechanism is an insignificant and impractical factor in most practical decision-making procedures – at least when based on the parameter ranges employed in this study. The land-surface slope has a minor impact on the overshoot values but leads to a differing time to reach them. A minor impact of land-surface slope on the overshoot mechanism agrees with the previous results of Morgan et al. (2013, 2015). The aquifer bed slope has also a small impact on the overshoot values while the associated effect is greater than the impact of land-surface slope.

Table 7
Comparison of the dimensionless seawater toe location changes predicted based on both the analytical solutions and the numerical simulation.

LWBCs	Land-surface slope (%)	Aquifer bed slope (%)	Numerical solution		Analytical solution[a]		Analytical solution[b]		Analytical solution[c]	
			ΔX^*_{Toe}[d]	R[e]	ΔX^*_{Toe}[d]	R[e]	ΔX^*_{Toe}[d]	R[e]	ΔX^*_{Toe}[d]	R[e]
FC	0.5	0	0.219	1.4	0.285	5.5	0.290	5.2	0.340	6.3
FC	0.5	1	0.180	3.0	0.247	8.3	0.248	8.1	N/A	N/A
FC	5	0	0.116	0.3	0.068	0.5	0.071	0.5	0.075	0.6
FC	5	1	0.850	0.4	0.048	0.8	0.049	0.8	N/A	N/A
HC	0.5	0	~0.591	~0	N/A	N/A	N/A	N/A	N/A	N/A
HC	0.5	1	~0.660	~0	N/A	N/A	N/A	N/A	N/A	N/A
HC	5	0	~0.591	~0	N/A	N/A	N/A	N/A	N/A	N/A
HC	5	1	~0.655	~0	N/A	N/A	N/A	N/A	N/A	N/A

N/A: Not applicable.
[a] Based on Koussis et al. (2015), extended to consider the impacts of both SLR and the associated LSI in this study.
[b] Based on Koussis et al. (2012), extended to consider the impacts of both SLR and the associated LSI in this study.
[c] Based on Ataie-Ashtiani et al. (2013a) solution (applicable only for horizontal aquifer bed cases).
[d] The dimensionless SWI toe changes (the dimensionless value of difference between seawater toe location after SLR and prior to SLR).
[e] Ratio parameter to quantify the influence of LSI on SLR-induced SWI as $(X^s_{Toe} - X^v_{Toe})/(X^v_{Toe} - X^0_{Toe})$ (Ataie-Ashtiani et al., 2013a).

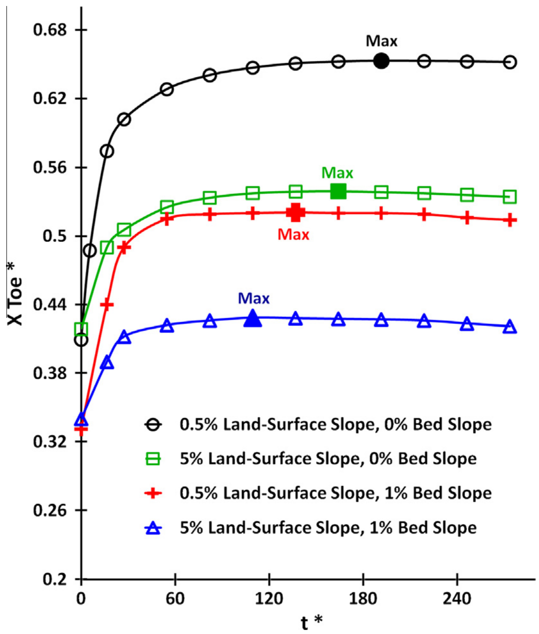

Fig. 10. Transient variations in X^*_{Toe} for the FC cases under a SLR of 1 m.

Table 8
The comparison of the overshoot mechanism behavior associated with a SLR of 1.

Land-surface slope (%)	Aquifer bed slope (%)	Steady-state X^*_{Toe}	Maximum		Reversal effect[a] (%)
			X^*_{Toe}	t^*	
0.5	0	0.652	0.653	192	0.16
0.5	1	0.534	0.539	164	0.91
5	0	0.514	0.521	137	1.26
5	1	0.421	0.429	110	1.78

[a] The percentage values are obtained based on the comparison of the steady-state and the maximum values of seawater toe location.

Our experiments for all HC cases indicate that the overshoot is not observed in these tests. Morgan et al. (2015) described the reasons of such observation. They concluded that while an approximately uniform head rise throughout the FC aquifer occurs due to SLR, for the HC case, a head rise reduces with distance from the coast and is zero at the landward boundary. Hence, the storage change after SLR is less under FC LWBCs compared to HC ones which leads to more rapid hydraulic re-equilibration and therefore no overshoot.

5.1.3. Seawater fingering due to SLR

The time series of the salinity distributions and flow directions with an instantaneous SLR of 1 m are presented in Fig. 11. The results show a vertical seawater column in which free convection develops as it intrudes downwards during the 10 days followed by a period of merging with the underlying lateral SWI. The seawater column begins mixing with the freshwater and seawater wedge before reaching the aquifer basement at later times (Fig. 11c–e). Below the inundated land surfaces, the strength of freshwater circulation is gradually reduced as a result of vertical flows induced by the fingering transport, as shown in Fig. 11c and d. After about 3 years, transient salinity fingering caused by LSI is almost completely finished. The new seawater toe location is formed when salinity fingers from the inundated land surface reach and mix with the horizontal SWI (seawater wedge). At this time (3 years), the seawater toe location reaches 430 m and after that, the horizontal intrusion of seawater will continue and reach 609 m and 628 m after 50 years and 100 years following SLR, respectively.

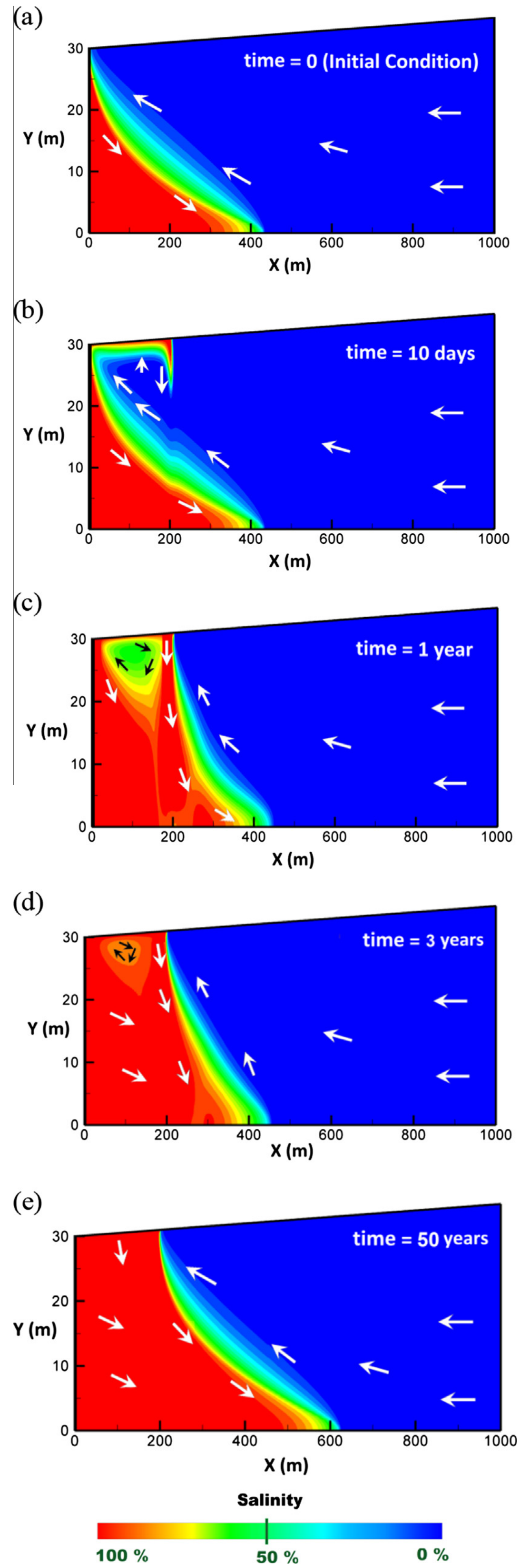

Fig. 11. The salinity distributions after a SLR of 1 m in the land-surface slope of 0.5% and FC LWBCs: (a) initial condition, (b) 10 days, (c) 1 year, (d) 3 years, and (e) 50 years.

6. Conclusions

In order to better understand the previous research, current knowledge gaps, and opportunities for advancing the understanding of SLR impacts on SWI in more general terms, we first conducted a literature review with a greater focus on SLR-induced phenomena and the associated impacts. Therefore, the first review of previous literature is provided in a diagrammatic and tabular form on SWI in coastal aquifers. This review demonstrates that all studies to date have only investigated a subset of known or anticipated controlling factors in their analyses. It is evident from the literature survey that there is a need to consider all of these purported controlling factors in a single, unifying, modeling framework in order to better understand the relative importance of these controlling factors as well as to progress a more general understanding of these controlling factors. Whilst this current study is demonstrative rather than exhaustive, it has yielded new insights on the gaps in current literature and the relative importance of all controlling factors. In addition, based on the review of literature, further work could include, for example, (1) including more realistic complexities such as considering the gradual SLR, topographic slopes, geologic heterogeneities, and pumping effects; (2) extending the research to real-world and large-scale cases; (3) a close examination of time-related phenomena such as overshoot and seawater fingers with more realistic assumptions such as gradual SLR; (4) undertaking a rigorous uncertainty analysis using e.g. Monte-Carlo simulations; and (5) implementing the impacts of climate change in decision-making models with the purpose of developing optimal groundwater management plans.

The review of the literature then, in turn, leads to the development of an integrated modeling study in which all purported controlling factors are included in both analytical and numerical models. The integrated impacts are studied by combining SLR, LSI caused by SLR, and variations in recharge rate on SWI in a sloping coastal aquifer under the different land-surface slopes, the aquifer bed slopes, and the LWBCs (the FC and HC systems) in addition to the investigation of time-related phenomena. This covers the key controlling factors documented in previous literature. Reasonable and realistic parameter ranges are assigned to each of these controlling factors to ensure that the results of this study are therefore representative and cover a range of broadly anticipated behavior in coastal region settings. The sharp-interface analytical solutions and the two-dimensional dispersive numerical simulations are performed. The key findings and conclusions of this study based on integrated assessments are:

1. The impact of LSI is the one of the most important stresses of SLR on the flatter aquifers. Due to the influence of LSI, a SWI increase is observed for the lower land-surface slopes. LSI relative impact is about an OoM larger in the FC cases compared to the HC ones. Also, the results obtained using dispersive numerical simulations demonstrate that LSI-induced SWI can be significantly less (about an OoM) than that of predicted by sharp-interface analytical solutions in coastal aquifers with realistic parameters.
2. The results highlight the importance of LWBCs on SLR impacts. The comparison of variations of the seawater toe location under two different LWBCs shows that the HC systems cause further SWI into inland in response to SLR compared with the FC systems.
3. A strong sensitivity of seawater toe location to fresh groundwater discharge to sea and recharge rate are observed for both FC and HC systems. Regional freshwater flux at the landward boundary and the groundwater hydraulic gradient provide the major source of fresh groundwater discharge to sea for FC and HC systems, respectively. Δh^*_{SW} is also an important factor with about an OoM smaller impact compared to the fresh groundwater discharge to sea and recharge rate parameters. The B^* impact for the HC cases is an OoM larger than that for the FC cases. The lowest sensitivities are found for δ and $\sin\varphi$ in both FC and HC cases.
4. Aquifer length has an insignificant impact on the seawater toe location due to SLR-LSI since the observed effects on a variety of aquifer lengths are almost similar. This response to SLR-LSI is greater for deeper aquifers under both FC and HC LWBCs although the HC systems are more sensitive to the aquifer thickness. It can be concluded that the important factor that significantly affects the response of aquifer is the ratio of the aquifer thickness to the aquifer length. The larger the ratio, the larger response of the aquifer and therefore larger seawater toe location changes.
5. The results of transient SWI behaviors confirm the occurrence of overshoot mechanism in the FC aquifers and no observation of it in the HC cases as documented by previous authors (e.g. Watson et al., 2010; Morgan et al., 2015). This mechanism has a smaller influence (lower than 2% reversal effect in comparison with steady-state status) when compared to all other controlling factors examined in this study. The maximum seawater toe location occurs at earlier times in higher land-surface and aquifer bed slopes. In addition, the approximate hundred year timescale of the overshoot mechanism and the relatively small spatial scales associated with it, lead to the conclusion that the overshoot mechanism is likely to be a less important factor for most practical purposes such as management decisions whose focus is climatic-induced changes in SWI.
6. The early-time observations show seawater fingers. As a result of free convection, the finger migrates downwards under gravitational influence. Seawater fingers begin mixing with the freshwater and horizontal SWI over time and below the inundated land surface, the freshwater circulation gradually reduces and eventually this phenomenon is diminished and ultimately extinguished. Early-time variations of SWI including free convection mechanism need to be evaluated further particularly in lower land-surface slopes that encounter larger LSI. This is because the occurrence of seawater fingers depends on the modes of SWI that can be influenced by some conditions such as instantaneous or gradual SLR in modeling procedure.

Acknowledgments

The author Craig T. Simmons acknowledges funding support of the National Centre for Groundwater Research and Training, a collaborative initiative of the Australian Research Council and the National Water Commission, Australia. The authors appreciate the constructive comments of the reviewer, Dr. Antonis D. Koussis, three anonymous reviewers, and Editor-in-Chief Dr. Geoff Syme, which helped to improve the final version of this paper.

References

Abarca, E., Carrera, J., Sanchez-Vila, X., Voss, C.I., 2007. Quasi-horizontal circulation cells in 3D seawater intrusion. J. Hydrol. 339, 118–129.
Ataie-Ashtiani, B., 2015. Comment on "Effects of tidal fluctuations on mixing and spreading in coastal aquifers: Homogeneous case" by María Pool et al. Water Resour. Res. 51 (6), 4858.
Ataie-Ashtiani, B., Ketabchi, H., 2011. Elitist continuous ant colony optimization algorithm for optimal management of coastal aquifers. Water Resour. Manage. 25, 165–190.
Ataie-Ashtiani, B., Ketabchi, H., Rajabi, M.M., 2014. Optimal management of freshwater lens in a small island using surrogate models and evolutionary algorithms. J. Hydrol. Eng. 19 (2), 339–354.

Ataie-Ashtiani, B., Werner, A.D., Simmons, C.T., Morgan, L.K., Lu, C., 2013a. How important is the impact of land-surface inundation on seawater intrusion caused by sea-level rise? Hydrogeol. J. 21 (7), 1673–1677.
Ataie-Ashtiani, B., Rajabi, M.M., Ketabchi, H., 2013b. Inverse modeling for freshwater lens in small islands: Kish Island, Persian Gulf. Hydrol. Process. 27, 2759–2773.
Ataie-Ashtiani, B., Volker, R.E., Lockington, D.A., 1999. Tidal effects on seawater intrusion in unconfined aquifers. J. Hydrol. 216 (1–2), 17–31.
Ataie-Ashtiani, B., Volker, R.E., Lockington, D.A., 2001. Tidal effects on groundwater dynamics in unconfined aquifers. Hydrol. Process. 15 (4), 655–669.
Bring, A., Asokan, S.M., Jaramillo, F., Jarsjö, J., Levi, L., Pietroń, J., Prieto, C., Rogberg, P., Destouni, G., 2015. Implications of freshwater flux data from the CMIP5 multi-model output across a set of Northern Hemisphere drainage basins. Earth's Future 3 (6), 206–217.
Carneiro, J.F., Boughriba, M., Correia, A., Zarhloule, Y., Rimi, A., El Houadi, B., 2010. Evaluation of climate change effects in a coastal aquifer in Morocco using a density-dependent numerical model. Environ. Earth Sci. 61 (2), 241–252.
Carretero, S., Rapaglia, J., Bokuniewicz, H., Kruse, E., 2013. Impact of sea-level rise on saltwater intrusion length into the coastal aquifer, partido dela costa, Argentina. Cont. Shelf Res. 61–62, 62–70.
Chang, S.W., Clement, T.P., 2012. Experimental and numerical investigation of saltwater intrusion dynamics in flux-controlled groundwater systems. Water Resour. Res. 48 (9), W09527.
Chang, S.W., Clement, T.P., Simpson, M.J., Lee, K.K., 2011. Does sea-level rise have an impact on saltwater intrusion? Adv. Water Resour. 34 (10), 1283–1291.
Chesnaux, R., 2015. Closed-form analytical solutions for assessing the consequences of sea-level rise on groundwater resources in sloping coastal aquifers. Hydrogeol. J. 23 (7), 1399–1413.
Ferguson, G., Gleeson, T., 2012. Vulnerability of coastal aquifers to groundwater use and climate change. Nat. Clim. Change 2 (5), 342–345.
Feseker, T., 2007. Numerical studies on saltwater intrusion in a coastal aquifer in northwestern Germany. Hydrogeol. J. 15 (2), 267–279.
Green, N.R., MacQuarrie, K.T.B., 2014. An evaluation of the relative importance of the effects of climate change and groundwater extraction on seawater intrusion in coastal aquifers in Atlantic Canada. Hydrogeol. J. 22 (3), 609–623.
Giambastiani, B., Antonellini, M., Oude Essink, G.H., Stuurman, R.J., 2007. Saltwater intrusion in the unconfined coastal aquifer of Ravenna (Italy): a numerical model. J. Hydrol. 340 (1), 91–104.
Gorelick, S.M., Zheng, C., 2015. Global change and the groundwater management challenge. Water Resour. Res. 51, 3031–3051.
Holman, I.P., 2006. Climate change impacts on groundwater recharge-uncertainty, shortcomings, and the way forward? Hydrogeol. J. 14 (5), 637–647.
Horton, B.P., Rahmstorf, S., Engelhart, S.E., Kemp, A.C., 2014. Expert assessment of sea-level rise by AD 2100 and AD 2300. Quatern. Sci. Rev. 84, 1–6.
International Panel on Climate Change (IPCC), 2007. Climate change 2007: impacts, adaptation and vulnerability. In: Parry, M.L., Canziani, O.F., Palutikof, J.P., van der Linden, P.J., Hanson, C.E. (Eds.), Contribution of Working Group II to the Fourth Assessment Report of the Intergovernmental Panel on Climate Change. Cambridge University Press, Cambridge.
International Panel on Climate Change (IPCC), 2013. Climate Change 2013: The Physical Science Basis. Working Group 1 Contribution to the Fifth Assessment Report of the International Panel on Climate Change. Cambridge, New York.
Ketabchi, H., Ataie-Ashtiani, B., 2015a. Evolutionary algorithms for the optimal management of coastal groundwater: a comparative study toward future challenges. J. Hydrol. 520, 193–213.
Ketabchi, H., Ataie-Ashtiani, B., 2015b. Review: coastal groundwater optimization—advances, challenges, and practical solutions. Hydrogeol. J. 23 (6), 1129–1154.
Ketabchi, H., Ataie-Ashtiani, B., 2015c. Assessment of a parallel evolutionary optimization approach for efficient management of coastal aquifers. Environ. Modell. Softw. 74, 21–38.
Ketabchi, H., Mahmoodzadeh, D., Ataie-Ashtiani, B., 2016. Groundwater travel time computation for two-layer islands. Hydrogeol. J. http://dx.doi.org/10.1007/s10040-015-1347-x.
Ketabchi, H., Mahmoodzadeh, D., Ataie-Ashtiani, B., Werner, A.D., Simmons, C.T., 2014. Sea-level rise impact on fresh groundwater lenses in two-layer small islands. Hydrol. Process. 28, 5938–5953.
Kooi, H., Groen, J., Leijnse, A., 2000. Modes of seawater intrusion during transgressions. Water Resour. Res. 36 (12), 3581–3589.
Koussis, A.D., Mazi, K., Riou, F., Destouni, G., 2012. Analytical single-potential, sharp interface solutions for regional seawater intrusion in sloping unconfined coastal aquifers, with pumping and recharge. J. Hydrol. 416–417, 1–11.
Koussis, A.D., Mazi, K., Riou, F., Destouni, G., 2015. A correction for Dupuit-Forchheimer interface flow models of seawater intrusion in unconfined coastal aquifers. J. Hydrol. 525, 277–285.
Laattoe, T., Werner, A.D., Simmons, C.T., 2013. Seawater intrusion under current sea-level rise: processes accompanying coastline transgression. In: Groundwater in the Coastal Zones of Asia-Pacific Coastal Research Library, vol. 7, pp. 295–313.
Loaiciga, H.A., Pingel, T.J., Garcia, E.S., 2012. Seawater intrusion by sea-level rise: scenarios for the 21st century. Groundwater 50 (1), 37–47.
Lu, C., Werner, A.D., 2013. Timescales of seawater intrusion and retreat. Adv. Water Resour. 59, 39–51.
Lu, C., Xin, P., Li, L., Luo, J., 2015. Seawater intrusion in response to sea-level rise in a coastal aquifer with a general-head inland boundary. J. Hydrol. 522, 135–140.
Luoma, S., Okkonen, J., 2014. Impacts of future climate change and Baltic sea level rise on groundwater recharge, groundwater levels, and surface leakage in the Hanko aquifer in southern Finland. Water 6 (12), 3671–3700.
Mahmoodzadeh, D., Ketabchi, H., Ataie-Ashtiani, B., Simmons, C.T., 2014. Conceptualization of a fresh groundwater lens influenced by climate change: a modeling study of an arid-region island in the Persian Gulf, Iran. J. Hydrol. 519, 399–413.
Mazi, K., Koussis, A.D., Destouni, G., 2013. Tipping points for seawater intrusion in coastal aquifers under rising sea level. Environ. Res. Lett. 8, 014001.
Mazi, K., Koussis, A.D., Destouni, G., 2014. Intensively exploited Mediterranean aquifers: proximity to tipping points and control criteria for sea intrusion. Hydrol. Earth Syst. Sci. 18, 1663–1677.
Melloul, A., Collin, M., 2006. Hydrogeological changes in coastal aquifers due to sea level rise. Ocean Coast. Manage. 49, 281–297.
Michael, H.A., Russoniello, C.J., Byron, L.A., 2013. Global assessment of vulnerability to sea-level rise in topography-limited and recharge-limited coastal groundwater systems. Water Resour. Res. 49 (4), 2228–2240.
Moe, H., Hossain, R., Fitzgerald, R., Banna, M., Mushtaha, A., Yaqubi, A., 2001. Application of 3-dimensional coupled flow and transport model in the Gaza Strip. In: First International Conference on Saltwater Intrusion and Coastal Aquifers-Monitoring, Modeling, and Management, Essaouira, Morocco, April 23–25, 2001.
Morgan, L.K., Bakker, M., Werner, A.D., 2015. Occurrence of seawater intrusion overshoot. Water Resour. Res. 51 (4), 1989–1999.
Morgan, L.K., Werner, A.D., 2014. Seawater intrusion vulnerability indicators for freshwater lenses in strip islands. J. Hydrol. 508, 322–327.
Morgan, L.K., Stoeckl, L., Werner, A.D., Post, V.E.A., 2013. An assessment of seawater intrusion overshoot using physical and numerical modeling. Water Resour. Res. 49 (10), 6522–6526.
Ojha, R., Ramadas, M., Govindaraju, R., 2015. Current and future challenges in groundwater I: modeling and management of resources. J. Hydrol. Eng. Special Issue: Grand Challenges Hydrol., A4014007
Oude Essink, G.H.P., Van Baaren, E.S., De Louw, P.G.B., 2010. Effects of climate change on coastal groundwater systems: a modeling study in the Netherlands. Water Resour. Res. 46, W00F04.
Pool, M., Carrera, J., 2011. A correction factor to account for mixing in Ghyben-Herzberg and critical pumping rate approximations of seawater intrusion in coastal aquifers. Water Resour. Res. 47, W05506.
Rajabi, M.M., Ataie-Ashtiani, B., 2014. Sampling efficiency in Monte Carlo based uncertainty propagation strategies: application in seawater intrusion simulations. Adv. Water Resour. 67, 46–64.
Rajabi, M.M., Ataie-Ashtiani, B., Simmons, C.T., 2015a. Polynomial chaos expansions for uncertainty propagation and moment independent sensitivity analysis of seawater intrusion simulations. J. Hydrol. 520, 101–122.
Rajabi, M.M., Ataie-Ashtiani, B., Janssen, H., 2015b. Efficiency enhancement of optimized Latin hypercube sampling strategies: application to Monte Carlo uncertainty analysis and meta-modeling. Adv. Water Resour. 76, 127–139.
Rasmussen, P., Sonnenborg, T.O., Goncear, G., Hinsby, K., 2013. Assessing impacts of climate change, sea level rise, and drainage canals on saltwater intrusion to coastal aquifer. Hydrol. Earth Syst. Sci. 17 (1), 421–443.
Rotzoll, K., Fletcher, C.H., 2012. Assessment of groundwater inundation as a consequence of sea-level rise. Nat. Clim. Change 3 (5), 477–481.
Sefelnasr, A., Sherif, M., 2014. Impacts of seawater rise on seawater intrusion in the Nile delta aquifer, Egypt. Groundwater 52 (2), 264–276.
Sherif, M.M., Singh, V.P., 1999. Effect of climate change on sea water intrusion in coastal aquifers. Hydrol. Process. 13 (8), 1277–1287.
Sreekanth, J., Datta, B., 2014. Stochastic and robust multi-objective optimal management of pumping from coastal aquifers under parameter uncertainty. Water Resour. Manage. 28 (7), 2005–2019.
Stigter, T.Y., Nunes, J.P., Pisani, B., Fakir, Y., Hugman, R., Li, Y., Tome, S., Ribeiro, L., Samper, J., Oliveira, R., Monteiro, J.P., Silva, A., Tavares, P.C.F., Shapouri, M., Cancela da Fonseca, L., El Himer, H., 2014. Comparative assessment of climate change and its impacts on three coastal aquifers in the Mediterranean. Reg. Environ. Change 14 (1), 41–56.
Strack, O.D.L., 1976. A single-potential solution for regional interface problems in coastal aquifers. Water Resour. Res. 12, 1165–1174.
Terry, J.P., Falkland, A.C., 2010. Responses of atoll freshwater lenses to storm-surge overwash in the Northern Cook Islands. Hydrogeol. J. 18 (3), 749–759.
Van der Veer, P., 1977. Analytical solution for steady interface flow in a coastal aquifer involving a phreatic surface with precipitation. J. Hydrol. 34, 1–11.
Voss, C.I., Provost, A.M., 2010. SUTRA: A Model for Saturated–Unsaturated, Variable Density Roundwater Flow with Solute or Energy Transport. USGS Water-Resources Investigations Report, 02-4231, U.S. Geological Survey, Reston, VA.
Voss, C.I., Souza, W.R., 1987. Variable density flow and solute transport simulation of regional aquifers containing a narrow freshwater-seawater mixing zone. Water Resour. Res. 23 (10), 1851–1866.
Watson, A., Werner, A.D., Simmons, C.T., 2010. Transience of seawater intrusion in response to sea level rise. Water Resour. Res. 46 (12), W12533, 10 pp.
Webb, M.D., Howard, K.W., 2011. Modeling the transient response of saline intrusion to rising sea-levels. Groundwater 49 (4), 560–569.

Werner, A.D., Bakker, M., Post, V.E.A., Vandenbohede, A., Lu, C., Ataie-Ashtiani, B., Simmons, C.T., Barry, D.A., 2013. Seawater intrusion processes, investigation and management: recent advances and future challenges. Adv. Water Resour. 51 (1), 3–26.

Werner, A.D., Gallagher, M.R., 2006. Characterization of seawater intrusion in the Pioneer Valley, Australia using hydrochemistry and three-dimensional numerical modeling. Hydrogeol. J. 14 (8), 1452–1469.

Werner, A.D., Simmons, C.T., 2009. Impact of sea-level rise on seawater intrusion in coastal aquifers. Groundwater 47 (2), 197–204.

Werner, A.D., Ward, J.D., Morgan, L.K., Simmons, C.T., Robinson, N.I., Teubner, M.D., 2012. Vulnerability indicators of sea water intrusion. Groundwater 50 (1), 48–58.

Wheater, H.S., Mathias, S.A., Li, X., 2010. Groundwater Modeling in Arid and Semi-arid Areas. Cambridge University Press.

Yechieli, Y., Shalev, E., Wollman, S., Kiro, Y., Kafri, U., 2010. Response of the Mediterranean and Dead Sea coastal aquifers to sea level variations. Water Resour. Res. 46, W12550.